

## **Establishing Default Dynamic Modulus Values For New England**

Eric Jackson, Ph.D.  
Jingcheng Li  
Adam Zofka, Ph. D.  
IliyaYut, M. S.  
James Mahoney M.S.

**Prepared for  
The New England Transportation Consortium  
April 11, 2011**

**NETCR85**

**NETC06-3**

*This report, prepared in cooperation with the New England Transportation Consortium, does not constitute a standard, specification, or regulation. The contents of this report reflects the view of the authors who are responsible for the facts and the accuracy of the data presented herein. The contents do not necessarily reflect the views of the New England Transportation Consortium or the Federal Highway Administration.*

## **ACKNOWLEDGEMENTS**

The following are the members of the Technical Committee that developed the scope of work for the project and provided technical oversight throughout the course of the research:

David Kilpatrick, Connecticut Department of Transportation, Chairperson  
Stephen Cooper, Federal Highway Administration-CT Division  
Jeffrey DiFilippo, Rhode Island Department of Transportation  
Edmund Naras, Massachusetts Department of Transportation  
Timothy Soucie, Maine Department of Transportation  
Eric Thibodeau, New Hampshire Department of Transportation

## Technical Report Documentation Page

1 Report No. NETCR85	2. Government Accession No. N/A	3. Recipient's Catalog No. N/A	
4. Title and Subtitle Establishing Default Dynamic Modulus Values For New England		5. Report Date April 11, 2011	
		6. Performing Organization Code N/A	
7. Authors Eric Jackson, Ph.D. Jingcheng Li Adam Zofka, Ph. D. IliyaYut, M.S. James Mahoney, M.S.		8. Performing Organization Report No. NETCR85	
9. Performing Organization Name and Address University of Connecticut Connecticut Advanced Pavement Laboratory Storrs, CT 06269		10. Work Unit No (TRAIS) N/A	
		11. Contract or Grant No. N/A	
12. Sponsoring Agency name and Address New England Transportation Consortium University of Massachusetts Dartmouth 151 Martine Street Fall River, MA 02723		13. Type of Report and Period Covered Final Report	
		14. Sponsoring Agency Code NETC 06-3 A Study conducted in cooperation with the US DOT	
15. Supplementary Notes N/A			
16. Abstract.  The primary objective of this research is to test commonly used Hot Mix Asphalt (HMA) mixtures throughout New England to determine their respective dynamic modulus master curves. Four mixes were requested from each of the New England states for modulus testing. Physical testing consisted of two replicates of each mix, outfitted with 3, linear variable differential transformers (LVDTs). AASHTO TP 62 was followed for the testing of these samples. Comparisons of plant produced mix vs. lab produced mix shows no significant difference between the two methods. Thus indicating lab produced samples are analogous to real-world pavements for dynamic modulus testing. Furthermore, the results of physical modulus testing were compared to predicted modulus values from three different theoretical modulus models. Comparisons of Predicted  E*  values from the Mechanistic-Empirical Pavement Design Guide (MEPDG) and physical testing indicates the predicted  E*  values may be off by as much as 100% for New England Mixes. Through this research scaling factors were developed for all the mixes tested to allow state DOTs to forgo expensive and labor intensive physical testing. Furthermore, the minimal range and standard deviation of scaling factors for the Hirsh and Witczak models indicates there is potentially a constant scaling factor that could be applied to all New England mixes, regardless of aggregate source, and binder type. However, further testing may be required to determine if a uniform scaling factor for our region is truly valid.			
17. Key Words: Dynamic Modulus Hot Mix Asphalt (HMA) Mechanistic-Empirical Pavement Design Software (MEPDS) Master Curves AASHTO TP 62		18. Distribution Statement No restrictions. This document is available to the public through the National Technical Information Service Springfield, Virginia 2216	
19. Security Classif. (of this report)  Unclassified	20. Security Classif. (of this page)  Unclassified	21. No. of pages  79	22. Price  N/A

Form DOT F 1700.7 (8-72)

Reproduction of completed page authorized

# SI\* (MODERN METRIC) CONVERSION FACTORS

## APPROXIMATE CONVERSIONS TO SI UNITS

Symbol	When You Know	Multiply By	To Find	Symbol	When You Know	Multiply By	To Find	Symbol
--------	---------------	-------------	---------	--------	---------------	-------------	---------	--------

### LENGTH

in	inches	25.4	millimetres	mm
ft	feet	0.305	metres	m
yd	yards	0.914	metres	m
mi	miles	1.61	kilometres	km
<u>AREA</u>				
in <sup>2</sup>	square inches	645.2	millimetres squared	mm <sup>2</sup>
ft <sup>2</sup>	square feet	0.093	metres squared	m <sup>2</sup>
yd <sup>2</sup>	square yards	0.836	metres squared	m <sup>2</sup>
ac	acres	0.405	hectares	ha
mi <sup>2</sup>	square miles	2.59	kilometres squared	km <sup>2</sup>

### VOLUME

fl oz	fluid ounces	29.57	millilitres	mL
gal	gallons	3.785	Litres	L
ft <sup>3</sup>	cubic feet	0.028	metres cubed	m <sup>3</sup>
yd <sup>3</sup>	cubic yards	0.765	metres cubed	m <sup>3</sup>

NOTE: Volumes greater than 1000 L shall be shown in m<sup>3</sup>

### MASS

oz	ounces	28.35	grams	g
lb	pounds	0.454	kilograms	kg
T	short tons (2000 lb)	0.907	megagrams	Mg

### TEMPERATURE (exact)

°F	Fahrenheit temperature	5(F-32)/9	Celsius temperature	°C
----	------------------------	-----------	---------------------	----

### LENGTH

mm	millimetres	0.039	inches	in
m	metres	3.28	feet	ft
m	metres	1.09	yards	yd
km	kilometres	0.621	miles	mi
<u>AREA</u>				
mm <sup>2</sup>	millimetres squared	0.0016	square inches	in <sup>2</sup>
m <sup>2</sup>	metres squared	10.764	square feet	ft <sup>2</sup>
ha	hectares	2.47	acres	ac
km <sup>2</sup>	kilometres squared	0.386	square miles	mi <sup>2</sup>

### VOLUME

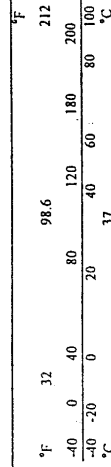
mL	millilitres	0.034	fluid ounces	fl oz
L	litres	0.264	gallons	gal
m <sup>3</sup>	metres cubed	35.315	cubic feet	ft <sup>3</sup>
m <sup>3</sup>	metres cubed	1.308	cubic yards	yd <sup>3</sup>

### MASS

g	grams	0.035	ounces	oz
kg	kilograms	2.205	pounds	lb
Mg	megagrams	1.102	short tons (2000 lb)	T

### TEMPERATURE (exact)

°C	Celsius temperature	1.8C+32	Fahrenheit temperature	°F
----	---------------------	---------	------------------------	----



\* SI is the symbol for the International System of Measurement

## *List of Abbreviations*

DOT	Departments of Transportation
AASHTO	American Association of State Highway and Transportation Officials
MEPDG	Mechanistic-Empirical Pavement Design Guide
MEPDS	Mechanistic-Empirical Pavement Design Software
HMA	Hot mix asphalt
SPT	Simple performance tester
AMPT	Asphalt mixture performance tester
$ E^* $	Dynamic modulus
ODB	Olard-Di Benedetto Model
VMA	Voids in the mineral aggregate
VFA	Voids filled with asphalt
DSR	Dynamic shear rheometer
LVDT	Linear variable differential transducer
VA	Voids in aggregate
NMAS	Nominal Maximum Aggregate Size
RAP	Recycled asphalt pavement

## TABLE OF CONTENTS

Acknowledgements.....	ii
Technical Documents Page.....	iii
SI Conversion Factors.....	iv
List of Abbreviations .....	v
Table of Contents.....	vi
List of Tables and Figures.....	vii
1.0 Introduction.....	1
2.0 Objectives and research approach.....	2
3.0 Background.....	2
3.1 The Witczak Model.....	4
3.2 The Hirsch Model .....	5
3.3 The Olard-Di Benedetto Model (ODB).....	6
3.4 Factors Influencing $ E^* $ .....	6
4.0 Research Approach.....	7
4.1 Specimen Collection and Fabrication.....	7
4.2 Dynamic Modulus Testing.....	8
5.0 Results.....	9
5.1 Master Curve Development.....	9
5.2 Comparison of Laboratory and Plant Produced Mixes.....	13
5.3 Reduced Physical Modulus Testing.....	16
5.4 Master Curve Predictions Using Mix and Binder Specifications.....	17
6.0 Conclusions.....	23
6.1 New England Mix Conclusions .....	23
6.2 Lab vs Plant Conclusions.....	24
6.3 Reduced Testing Curve Comparison .....	24
6.4 Measured vs Predicted $ E^* $ Comparison .....	25
7.0 References.....	26
Appendix A: Mix and State Specific Master Curves.....	29
Appendix B: AASHTO TP-62 Master Curves vs Reduced Testing Master Curves .....	48
Appendix C: Predicted vs Measured $ E^* $ .....	54

*List of Tables*

Table 1: Mixes Provided for Testing.....8  
Table 2: Dynamic Modulus Testing Specifications.....9  
Table 3: Model Scale Factors.....20  
Table 4: Percent Error Reduction Pre and Post Scale Factors Applied.....21

*List of Figures*

Figure 1: Master Curves for Connecticut Mixes.....10  
Figure 2: Master Curves for Maine Mixes.....11  
Figure 3: Master Curves for New Hampshire Mixes.....11  
Figure 4: Master Curves for Rhode Island Mixes.....12  
Figure 5: Master Curves for Vermont Mixes.....12  
Figure 6: Plant Vs Lab Master Curve Comparison.....14  
Figure 6 (Cont.): Plant Vs Lab Master Curve Comparison.....15  
Figure 6 (Cont.): Plant Vs Lab Master Curve Comparison.....16  
Figure 7: Predicted Vs Tested  $|E^*|$  Values (MPa) (linear scale) (CT A 12.5 mm).....19  
Figure 8: Log-Log Plot of Predicted Vs Tested  $|E^*|$  Values (MPa) (CT A 12.5 mm).....19  
Figure 9: Scaled Predicted Vs Tested  $|E^*|$  Values (MPa) (linear scale) (CT A 12.5 mm).....22  
Figure 10: Log-Log Plot of Scaled Predicted Vs Tested  $|E^*|$  Values (MPa) (CT A 12.5 mm)....22  
Figure 11: State-by-State Comparison of 12.5mm, 64-28, 15% RAP Mixes.....24  
Figure B1: Full and Reduced Testing Master Curves For Connecticut Mixes.....49  
Figure B2: Full and Reduced Testing Master Curves For Maine Mixes.....50  
Figure B3: Full and Reduced Testing Master Curves For New Hampshire Mixe.....51  
Figure B4: Full and Reduced Testing Master Curves For Rhode Island Mixes.....52  
Figure B5: Full and Reduced Testing Master Curves For Vermont Mixes.....53

## 1.0 INTRODUCTION

Departments of Transportation (DOT) spend hundreds of millions of dollars every year on design, construction, and rehabilitation of asphalt pavements. Most of the design procedures are based on 1986 and 1993 American Association of State Highway and Transportation Officials (AASHTO) design guides (AASHTO 1986, AASHTO 1993), which are primarily empirical in nature. These AASHTO guides were developed on the basis of field tests conducted in Illinois in the 1960's. Results from these field tests are not applicable for a different climatic region, and also for today's traffic and construction materials. Furthermore, significant changes in layer properties occur as a result of change in seasons, and it is critical that such changes are determined, documented, and considered properly for design, construction, and load restrictions. Although the mechanistic-empirical pavement design procedure has been in use in many forms for a long time, the recently developed Mechanistic-Empirical Pavement Design Software (MEPDS) and Guide (NCHRP 1-37A) (henceforth referred to as the 2002 MEPDG) represent the results of the first comprehensive national-level effort for implementation of this procedure in the US. The 2002 MEPDG covers both asphalt and concrete pavement design. These designs use algorithms based upon variables such as pavement structure, climate, anticipated traffic loadings, properties of the materials to be used in the pavement as well as base and sub-base properties to predict pavement performance. The 2002 MEPDG has three levels of pavement design. Level 3 requires the least amount of laboratory testing of the pavement materials and would generally be used for pavements in areas with the least amounts of traffic. The level of materials testing increases with a decrease in level number. Level 2 MEPDG testing uses specified inputs and the Witczak model evaluated as part of this research. Level 1 pavement design requires the greatest amount of testing to be performed. This includes performing the dynamic modulus testing on the proposed materials to be used for the hot mix asphalt (HMA) pavement.

The MEPDG is a comprehensive reference guide for the MEPDS, including information on flexible and rigid pavement design. It discusses all applicable variables involved with the design of roadway structures, including the material properties of HMA, base, and sub base layers. The guide incorporates discussions on the causes and practical methods of prevention of commonly experienced distresses. Steps for each process, applicable equations, some default values, and background information regarding the results of each test are included in the guide. The MEPDS can be used to simulate pavement structures with various options and inputs for relevant volumetric and stiffness properties. Using this software, engineers have the ability to determine the effect of using different types of materials through simulations and hence determine the optimum combination of materials and structure. The most important property needed for HMA is its stiffness.

The specific parameter suggested for representing the stiffness of HMA is its dynamic modulus,  $|E^*|$  (AASHTO TP 62).  $|E^*|$  is defined as the absolute value of the complex modulus calculated by dividing the maximum (peak to peak) stress by the recoverable (peak to peak) axial strain from a material subjected to a sinusoidal loading, where complex modulus,  $E^*$  is defined as a complex number that defines the relationship between stress and strain for a linear viscoelastic material (AASHTO TP 62). Therefore, dynamic (complex) modulus,  $E^*$ , could be considered one of the most important HMA properties influencing the structural response of a flexible pavement. The  $|E^*|$  determines the ability of material to resist compressive deformation as it is subjected to cyclic compressive loading and unloading. Furthermore,  $|E^*|$  is selected as

the required input to compute stresses and strains in HMA pavement (NCHRP 1-37A). As part of NCHRP Projects 9-19 (Superpave Support and Performance Models Management) and 9-29 (Simple Performance Tester for Superpave Mix Design), a simple performance tester (SPT) now called the asphalt mixture performance tester (AMPT) has been proposed to verify the performance characteristics (e.g., fatigue and rutting resistance) of Superpave mixture designs (Bonaquist et. al, 2003, Witczak, 2005). Remarkable effort has been done to predict  $|E^*|$  for asphalt mixes using two approaches. The analytical approach predicts  $|E^*|$  using numerical and analytical modeling, while the empirical approach predicts  $|E^*|$  using models based on correlation of SPT/AMPT test results with the physical and mechanical properties of binder and mixes.

## 2.0 OBJECTIVES AND RESEARCH APPROACH

The objective of this research is to test commonly used HMA mixtures throughout New England to determine their respective moduli. The results of this testing will be:

- Used to determine if there is a significant difference between dynamic modulus values for materials from throughout the region.
- Used to compare the dynamic modulus of lab produced mixes and plant produced mixes.
- Compared against the master curves derived by performing the reduced testing as outlined by Bonaquist and Christensen (2005). This will reduce the number of temperatures as well as the number of frequencies tested. If this process correlates well with the full set testing master curves, it will reduce the amount of time required to conduct the testing.
- Compare lab measured  $|E^*|$  against the predictive moduli obtained by using the Witczak Predictive Model, the Hirsh Model and the Olard-Di Benedetto (ODB) model. If there is a strong correlation between the tested and predicted values then this would provide a reasonable value for the dynamic modulus for most HMA designs in the 2002 Pavement Design Guide.

## 3.0 BACKGROUND

The dynamic modulus ( $|E^*|$ ) is defined as a complex number that relates stress to strain for linear viscoelastic materials subjected to continuously applied sinusoidal loading in the frequency domain. The absolute value of the complex modulus,  $\|E^*\|$  is generally referred to as the dynamic modulus.

Under the NCHRP Projects 9-19 and 9-29, the AMPT test was developed to provide fundamental engineering properties of asphalt mixtures (Bonaquist et al, 2003,Witczak, 2005). The Standard Method of Test for Determining Dynamic Modulus of Hot-Mix Asphalt Concrete Mixtures (AASHTO TP 62-03) was originally released in 2004 (AASHTO, 2010). This test method covers procedures for preparing and testing asphalt concrete mixtures to determine the  $|E^*|$  and phase angle over a range of temperatures and loading frequencies.

A full characterization of asphalt mixtures requires one to construct a master curve, which defines the viscoelastic material behavior as a function of both temperature and loading time or frequency. The master curve is constructed based on dynamic modulus and the phase angle values obtained from the test data over a range of temperatures and frequencies employing the principle of time-temperature superposition (Shaw and Macknight, 2005).

According to the MEPDG procedure, the modulus of the asphalt concrete at all levels of temperature and time rate loading is determined from a master curve. To construct a master curve, the reference temperature must be selected first, generally 70 °F (21.1°C), then  $|E^*|$  data collected at different temperatures should be shifted with respect to the time of loading or frequency. The shift factor needed at each temperature is constant for a given temperature (NCHRP 1-37A). Another shifting method is the Gordon and Shaw free-shifting method (Gordon and Shaw, 1994).

The new MEPDG used  $|E^*|$  values determined from a master curve constructed from measurements at multiple temperatures and loading time. The levels of temperature and time rate of load are determined from a sigmoid shaped master curve. A sigmoid function is symmetric which is consistent with the limitations of  $|E^*|$  values at temperature, aging and loading rate (Rowe et al., 2008). The master curve is mathematically modeled by a sigmoid function described as follows:

$$\log E^* = \delta + \frac{\alpha}{1 + e^{\beta + \gamma(\log t_r)}} \quad (1)$$

where:

- $t_r$  = reduced time of loading at reference temperature
- $\delta$  = minimum value of  $|E^*|$
- $\delta + \alpha$  = maximum value of  $|E^*|$
- $\beta, \gamma$  = parameters describing the shape of the sigmoid function

The shift factor is defined as follows:

$$a(T) = \frac{t}{t_r} \quad (2)$$

where

- $a(T)$  = shift factor as a function of temperature
- $t$  = time of loading at desired temperature
- $t_r$  = reduced time of loading at reference temperature
- $T$  = temperature of interest

The Gordon and Shaw free-shifting method uses a model-independent shift. It requires reasonable quality of data with sufficient number of data points (i.e. measurements at 6 temperature levels and at least 10 frequencies). The master curve is constructed using a pairwise shift centered on reference temperature (Gordon and Shaw, 1994). In this study, the Gordon-Shaw method was employed to create the master curve for each mix. The shifting procedure was automated using computational code created in MATLAB® 7.6.0 environment (MATLAB, 2009).

As the complex modulus test is relatively difficult and expensive to perform, numerous attempts have been made to develop regression equations to calculate the dynamic modulus from conventional binder and mixture properties. There are several models to predict dynamic modulus of asphalt concrete. Three of them are discussed below in the following order: The revised Andrei-Witczak model developed for MEPDG (NCHRP 1-37A), the modified Hirsch model proposed by Christensen et al. (2003), and the ODB model (Di Benedetto et. al, 2004, Olard and Di Benedetto, 2003).

### 3.1 The Witczak Model

The original version of the  $|E^*|$  predictive equation was developed by Shook and Kalas in the late 1960s (Shook and Kallas, 1969). Fonseca and Witczak (1996) further modified and refined a predictive model over years through the use of a database of hundreds of measurements. The Witczak equation has the form of a sigmoid function with the lower and upper bounds equal to  $\delta$  and  $(\delta+\alpha)$  respectively (See Equation 1). The horizontal location of the transition zone and the slope in the master curve are defined by  $\beta$  and  $\gamma$ , respectively.

The first version of the Witczak predictive equation was included in NCHRP Project 1-37A in the New AASHTO Design Guide. In the MEPDG version 1.0 release, a revised predictive equation for  $|E^*|$  is provided, as follows (Andrei *et al*, 1999):

$$\begin{aligned} \text{Log}|E^*| = & -1.249937 + 0.029232\rho_{200} - 0.001767(\rho_{200})^2 - 0.002841\rho_4 - 0.05809V_a \\ & - 0.802208 \left( \frac{V_{b\text{eff}}}{V_{b\text{eff}} + V_a} \right) + \frac{3.871977 - 0.002808\rho_4 + 0.003958\rho_{38} - 0.00001786(\rho_{38})^2 + 0.005470\rho_{34}}{1 + e^{(-0.603313 - 0.31335 \log(f) - 0.39353 \log(\eta))}} \end{aligned} \quad (3)$$

where

$|E^*|$  = dynamic modulus,  $10^5$  psi

$\eta$  = bitumen viscosity,  $10^6$  Poise

$f$  = loading frequency, Hz

$V_a$  = air void content, %

$V_{b\text{eff}}$  = effective bitumen content, % by volume

$\rho_{34}$  = cumulative % retained on the 19-mm (3/4) sieve

$\rho_{38}$  = cumulative % retained on the 9.5-mm (3/8) sieve

$\rho_4$  = cumulative % retained on the 4.76-mm (No. 4) sieve

$\rho_{200}$  = % passing the 0.075-mm (No. 200) sieve

The viscosity  $\eta$  is determined by the following equation:

$$\log \log \eta = A + VTS \log(T_R) \quad (4)$$

where:

$\eta$  = Newtonian viscosity, cP

$T_R$  = testing temperature, °Rankine

$A$  = regression intercept

$VTS$  = regression slope (viscosity-temperature susceptibility)

With introduction of the Superpave binder grading system based on Dynamic Shear Rheometer (DSR) testing for complex shear modulus,  $G^*$ , a new relationship between viscosity,  $\eta$ , and the Superpave binder rutting parameter  $|G^*| \sin \delta$  was developed, as shown below (UMA, 1998):

$$\eta = (|G^*|/\omega)(1/\sin \delta)^{(a_0 + a_1\omega + a_2\omega^2)} \quad (5)$$

where

$|G^*|$  = dynamic (complex) shear modulus

$\omega$  = angular frequency, rad/s  
 $\delta$  = phase angle  
 $a_0$  = fitting parameter = 3.639216  
 $a_1$  = fitting parameter = 0.131373  
 $a_2$  = fitting parameter = -0.000901

The revised predictive equation (Witczak, 2005) showed the best predictive strength in comparison with the previous model due to the use of more comprehensive database based on 7500 data points obtained from testing 366 mixes (Andrei et al, 1999). Nevertheless, the calibration of Witczak model seems to be necessary to account for differences in local climate and material sources.

### 3.2 The Hirsch Model

The original model was first developed by Hirsch (1961) to calculate the modulus of elasticity of Portland cement concrete based on empirical constant, the aggregate and cement mastic moduli, and mix proportions (Hirsh, 1961). Christensen et al.(2003) developed a relatively simple version based on Hirsch model to predict  $\|E^*\|$  of HMA from the complex shear modulus  $|G^*|$  of the asphalt binder, voids in the mineral aggregate (VMA), and voids filled with asphalt (VFA).

The phase angle of the HMA was predicted by a separate function based on the Hirsch model. Equations (Di Benedetto et. al, 2004) and (Olard and Di Benedetto, 2003) show the mathematical form of Hirsch model for HMA dynamic modulus (Andrei et al, 1999):

$$|E^*| = P_c \left[ 4200000 \left( 1 - \frac{VMA}{100} \right) + 3 |G^*|_{binder} \left( \frac{VFA \cdot VMA}{10000} \right) \right] + (1 - P_c) \left[ \frac{1 - \frac{VMA}{100}}{4200000} + \frac{VMA}{VFA \cdot 3 |G^*|_{binder}} \right] \quad (6)$$

$$P_c = \frac{\left( 20 + \frac{VFA \cdot 3 |G^*|_{binder}}{VMA} \right)^{0.58}}{650 + \left( \frac{VFA \cdot 3 |G^*|_{binder}}{VMA} \right)^{0.58}} \quad (7)$$

where

$\|E^*\|$  = dynamic modulus, psi  
 $|G^*|_{binder}$  = binder dynamic modulus, psi  
 $VMA$  = voids in the mineral aggregate, %  
 $VFA$  = voids filled with asphalt, %  
 $P_c$  = aggregate contact factor

The binder modulus  $|G^*|_{binder}$  can be determined experimentally using the dynamic shear rheometer (DSR) or a similar device or can be estimated from one of several mathematical models. It should be at the same temperature and loading time selected for the mixture modulus, and in consistent units (Andrei et al, 1999).

In recent years, the Witczak and Hirsch models have been extensively studied for comparison of prediction accuracy. Bonaquist and Christensen (2005) developed an alternative

procedure eliminating the low temperature from the SPT testing procedure, while estimating the limiting maximum modulus using the Hirsh model. Dongre et al. (2005) concluded that the Hirsh model reasonably estimates  $|E^*|$  at wider range of values than the Witczak model does. Nevertheless, both models underpredict  $|E^*|$  values when higher binder content or air voids than the mix design are present in production samples (Dongré et al., 2005). Finally, it is suspected that the Witczak equation may not be suitable for predicting  $|E^*|$  of polymer-modified binders (Dongré et al., 2005).

Birgisson et al (2005) examined the quality of the Witczak model  $|E^*|$  predictions for Florida. They found that Equation 3 can be used to predict measured  $|E^*|$  values with 85 to 90 percent reliability - if a multiplier used. Pellinen et al. (Pellinen et al., 2007) found that the Hirsch model, being a viscoelastic liquid model, is more flexible for further adjustments such as incorporating the creep behavior of mixture.

### 3.3 The Olard-Di Benedetto Model (ODB)

According to Di Benedetto et al. (2004), the linear viscoelastic properties of both asphalt binders and mixtures are predicted by the unique rheological model named the 2S2P1D model (Di Benedetto et. al, 2004, Olard and Di Benedetto, 2003), which is an acronym of two springs, two parabolic creep elements and one linear Newtonian dashpot. This model was developed as a generalization of the Huet-Sayegh analogical model with continuous spectrum (Di Benedetto et. al, 2004). Based on 2S2P1D model, Di Benedetto et al. developed a global analytical relationship between asphalt binder and the mixture complex moduli (Equation 8), which make their model stand apart from other prediction models (Pellinen et al., 2007).

$$E_{mix}^*(\omega, T) = E_{0\_mix} + \left[ E_{binder}^*(10^\alpha \omega, T) - E_{0\_binder} \right] \frac{E_{inf\_mix} - E_{0\_mix}}{E_{inf\_binder} - E_{0\_binder}} \quad (8)$$

This equation requires only three constants, static modulus ( $E_{0\_mix}$ ), glassy modulus, ( $E_{inf\_mix}$ ), and  $\alpha$ . The  $E_{0\_mix}$  and  $E_{inf\_mix}$  should be determined experimentally for a given mixture, whereas the parameter  $\alpha$  is dependent on the considered mix design and the aging (Di Benedetto et. al, 2004, Olard and Di Benedetto, 2003). In this study,  $\alpha = 2.82$  was used for any temperature, and the binder glassy modulus,  $E_{inf\_binder}$ , was estimated at 2.10 GPa for all binders, as suggested by Di-Benedetto et al. and other studies (Di Benedetto et. al, 2004, Olard and Di Benedetto, 2003, Pellinen et al., 2007). The static binder modulus  $E_{0\_binder}$  was assumed zero (Pellinen et al., 2007).

### 3.4 Factors Influencing $|E^*|$

Since an asphalt mixture is a composite material, its stiffness is governed, beside the external factors (traffic and climate), by the properties of the components (binder, aggregates, air voids and moisture).

The influence of loading configuration, aggregate distribution, and binder nonlinear viscoelastic properties on the dynamic modulus of asphalt mixtures have been examined by several studies. Birgisson et al (2005) concluded that the response of the mixture at high temperature (40°C) should be more dependent on the aggregate structure than at low temperature. Masad and Bahia (2002) found that the binder non-linear behavior is more prevalent under colder temperature and/or high-speed traffic. On the other hand, the asphalt

mixture non-linear behavior was detected at higher temperatures and/or lower frequencies, which is in contradiction to the trends observed in binders (Masad and Bahia, 2002).

With the increase in use of RAP material in the U.S., considerable research has been done on the effect of RAP on the mechanic properties of asphalt mixtures. At least two studies showed that, according to the indirect tension and semicircular bending tests, the addition of RAP increased the mixture stiffness (Huang et al., 2004, Li et al., 2008). Daniel and Vollmer (2005) studied the effect of increased RAP content (up to 40 percent) on the volumetric properties and stiffness of HMA (Daniel and Lachance, 2005). They found that increase in RAP content to 25 and even 40 percent is feasible without changing stiffness of the HMA mix at higher asphalt contents and a finer gradation (Daniel and Lachance, 2005).

Several studies confirmed a significant effect of the air void content on the HMA dynamic modulus. Seo et al. (2007) confirmed that increase in air voids results in lower  $|E^*|$  and shorter fatigue life of HMA mix and developed a model for predicting  $|E^*|$  values from air void content (Reo et al., 2007). Rowe et al. (2009) found the value of equilibrium and glassy modulus to be significantly affected by the volumetric properties of mixture (Rowe et al., 2009).

Bari and Witczak evaluated the effect of lime modification on the dynamic modulus stiffness of HMA by using the new MEPDG (Bari and Witczak, 2005). They found that lime-modified HMA mixtures on average had a 25% higher dynamic modulus than unmodified mixtures.

## **4.0 RESEARCH APPROACH**

### **4.1 Specimen Collection and Fabrication**

The research team requested each New England State Transportation Agency to identify four (4) mixes of their choosing to be used in this research project. For each of the mixes to be tested, the Transportation Agencies were asked to provide:

- respective mix designs (including nominal maximum aggregate size, gradation, asphalt binder source and grade);
- All aggregates for each mixture;
- Binder used in each mixture and;
- Plant mixed samples for one of requested mixes.

Once the material and mix designs were collected from each of the Transportation Agencies gyratory specimens were fabricated for both lab mixed specimens and plant produced specimens. Table 1 contains a list of specimens provided by each participating Transportation Agency. Specimens were compacted into cylinders with 170mm height and 150 mm diameter. These gyratory specimens were then cored and trimmed to obtain a test specimen 150 mm high and 100 mm in diameter. Each specimen was then tested (AASHTO T 269) to determine the percent air voids contained in the specimen. The target percent air voids for this project was  $4\% \pm 0.5$ . In order for a specimen to be accepted for testing the air voids must fall within this range. Samples that were outside this range were discarded and new samples were fabricated until two specimens for each state and each mix were successfully fabricated. The fabrication of these specimens was a very time and labor intensive trial and error process. Each mix required a different mass of material to produce a gyratory specimen with acceptable percent air voids for dynamic modulus testing. This process was employed for the lab mixed material and the respective plant produced mix.

Table 1: Mixes Provided for Testing

<b>State</b>	<b>Binder Grades</b>	<b>Mix Designation</b>	<b>NMAS</b>	<b>RAP Content</b>	<b>Superpave Level or ESAL's (millions)</b>
<b>VT</b>	PG58-28	VT A 9.5 mm	9.5mm	15%	4
		VT B 12.5 mm	12.5mm	0%	3
	PG64-28	VT C 12.5 mm	12.5mm	10%	3
		VT D 12.5 mm	12.5mm	15%	3
<b>NH</b>	PG64-28	NH B 9.5 mm	9.5mm	15%	1 ESALs
		NH A 12.5 mm	12.5mm	15%	>10 ESALs
		NH C 19 mm	19mm	15%	> 10 ESALs
		NH D 25 mm	25mm	15%	0.3 ESALs
<b>ME</b>	PG64-28	ME A 9.5 mm	9.5mm	15%	0.3 to <3 ESALs
		ME C 12.5 mm	12.5mm	15%	3 to <10 ESALs
		ME D 19 mm	19mm	0%	0.3 to <3 ESALs
<b>CT</b>	PG64-28	CT A 12.5 mm	12.5mm	0%	2
		CT B 12.5 mm			3
	PG64-28	CT C 12.5 mm	12.5mm	15%	2
		CT D 12.5 mm			3
<b>RI</b>	PG64-28	RI A M CL-1	12.5mm	0%	Marshall Mix CL-1
		RI C M CL-1			Marshall Mix CL-1
	PG76-28	RI B 12.5 mm	12.5mm	0%	1

#### **4.2 Dynamic Modulus Testing**

The Dynamic Modulus of each plant produced and lab mixed specimens were determined using AASHTO TP 62. The testing was performed using an IPC – Universal Testing Machine. Two replicate samples of each mix were fitted with 3 axial linear variable differential transducers (LVDTs). According to the accuracy charts in AASHTO TP 62 this should result in a modulus accuracy of  $\pm 13.1\%$ . Table 2 below describes the testing parameters used for each of the specimens.

Table 2: Dynamic Modulus Testing Specifications

Temp ( C )	Frequency (Hz)	Dynamic Stress (kPa)	Number of loading cycles
-10	25 Hz	2600	200
-10	10 Hz	2400	200
-10	5 Hz	2200	100
-10	1 Hz	2000	20
-10	0.5 Hz	1800	15
-10	0.1 Hz	1600	15
4	25 Hz	1300	200
4	10 Hz	1200	200
4	5 Hz	1100	100
4	1 Hz	1000	20
4	0.5 Hz	900	15
4	0.1 Hz	800	15
21	25 Hz	650	200
21	10 Hz	600	200
21	5 Hz	550	100
21	1 Hz	450	20
21	0.5 Hz	400	15
21	0.1 Hz	350	15
38.7	25 Hz	240	200
38.7	10 Hz	220	200
38.7	5 Hz	180	100
38.7	1 Hz	150	20
38.7	0.5 Hz	130	15
38.7	0.1 Hz	120	15
54	25 Hz	70	200
54	10 Hz	70	200
54	5 Hz	60	100
54	1 Hz	55	20
54	0.5 Hz	45	15
54	0.1 Hz	40	15

## 5.0 RESULTS

### 5.1 Master Curve Development

Based on the results of the modulus testing, a master curve was generated for each state's provided mixes. The reduced frequencies for the x-axis were calculated using Equation 2. To increase the precision of the shift factor a second order polynomial equation was used. Solving

for the appropriate shift factor, the reduced frequency can be plotted against the obtained modulus on a log-log scale. Then a sigmodal function (equation 1) can be generated to fit the resulting data as a function of reduced frequency. General master curves for each state can be found in Figures 1-5 below. Mix Specific master curves including an inset plot of shift factor can be found in Appendix A.

$$\log a(T_i) = aT_i^2 + bT_i + c \tag{9}$$

Where

$a(T_i)$  = Shift factor as a function of temperature  $T_i$   
 $T_i$  = Temperature of interest °F  
 a, b and c = Coefficients of the second order polynomial

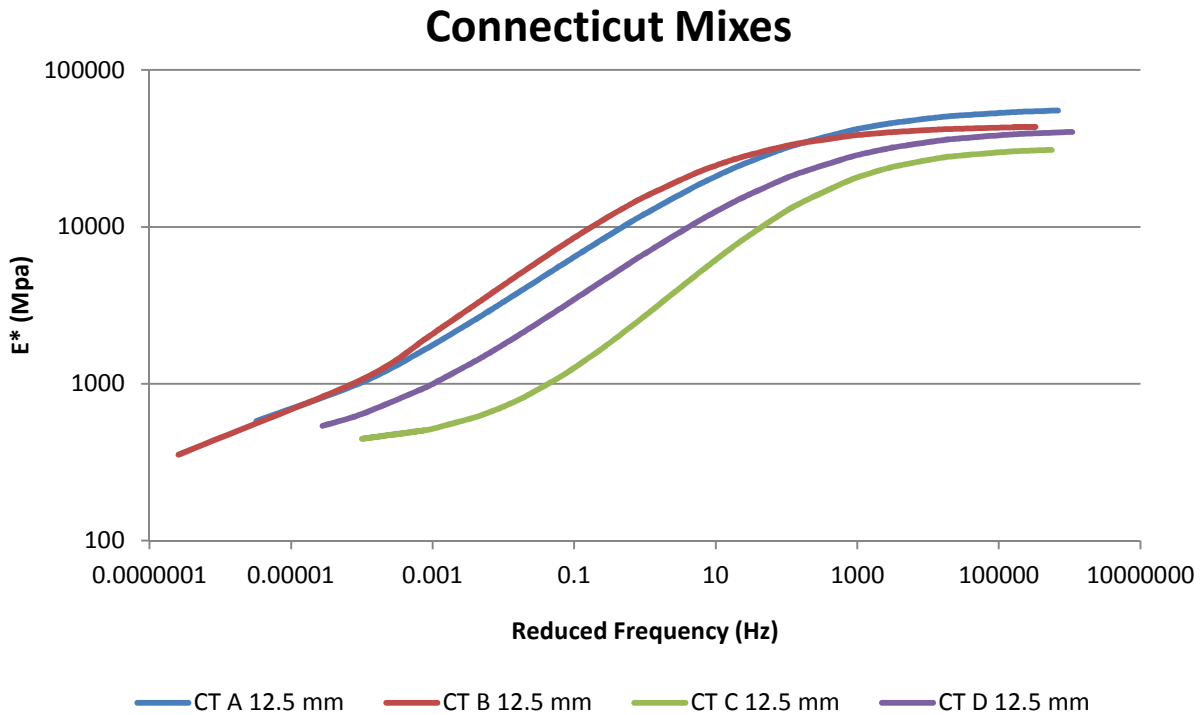


**Figure 1: Master Curves for Connecticut Mixes**

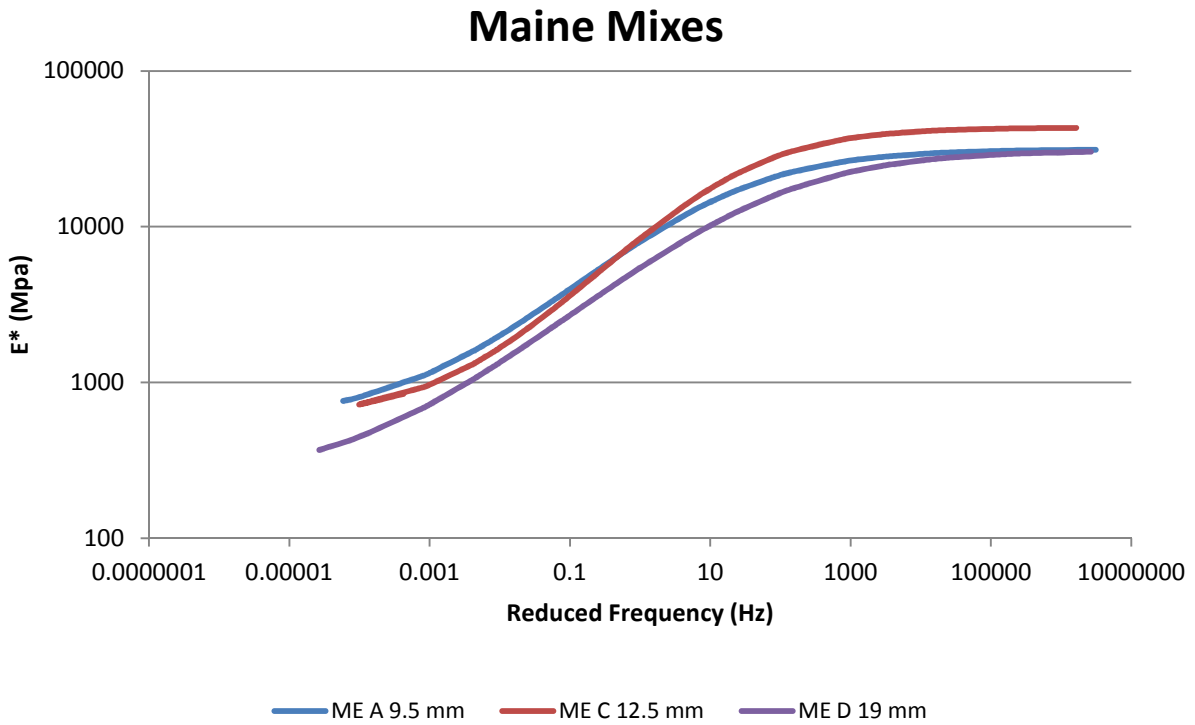


**Figure 2: Master Curves for Maine Mixes**

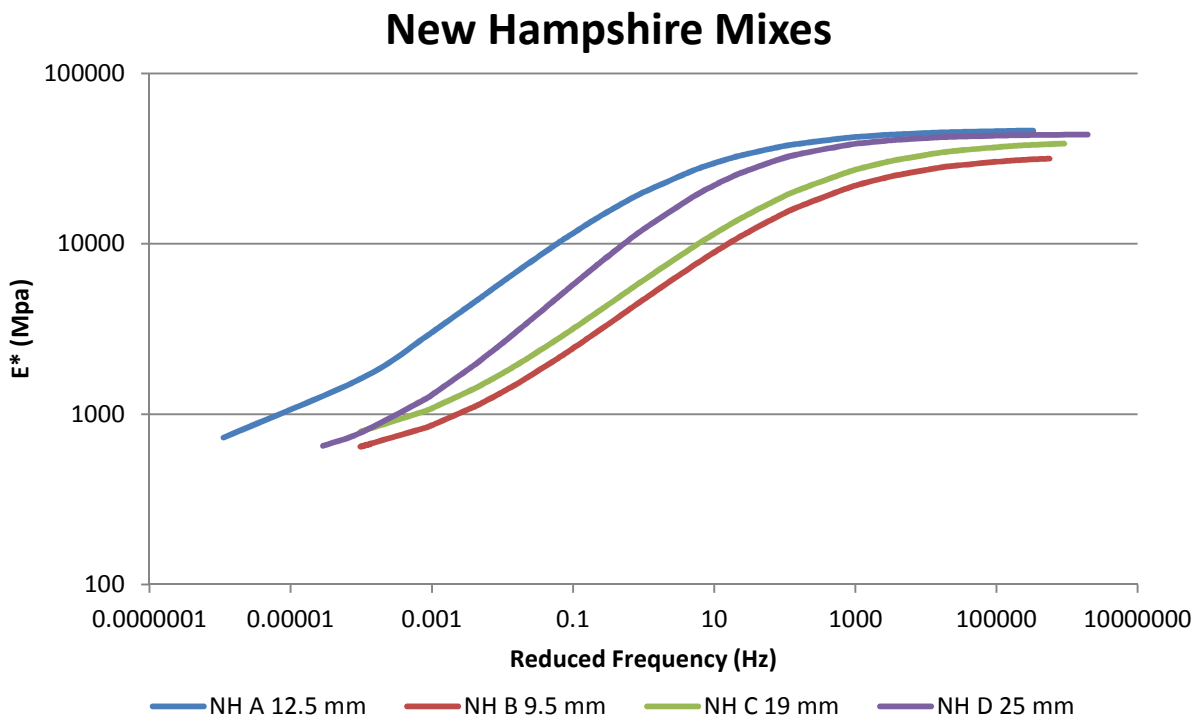


**Figure 3: Master Curves for New Hampshire Mixes**

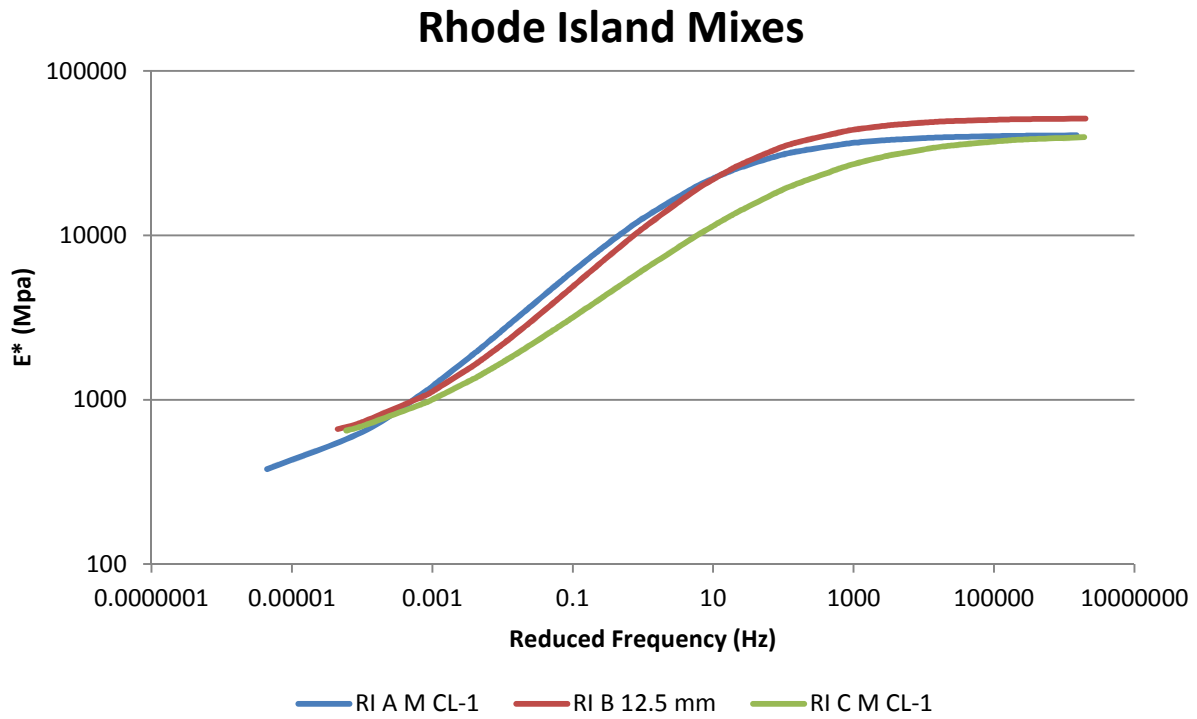


**Figure 4: Master Curves for Rhode Island Mixes**

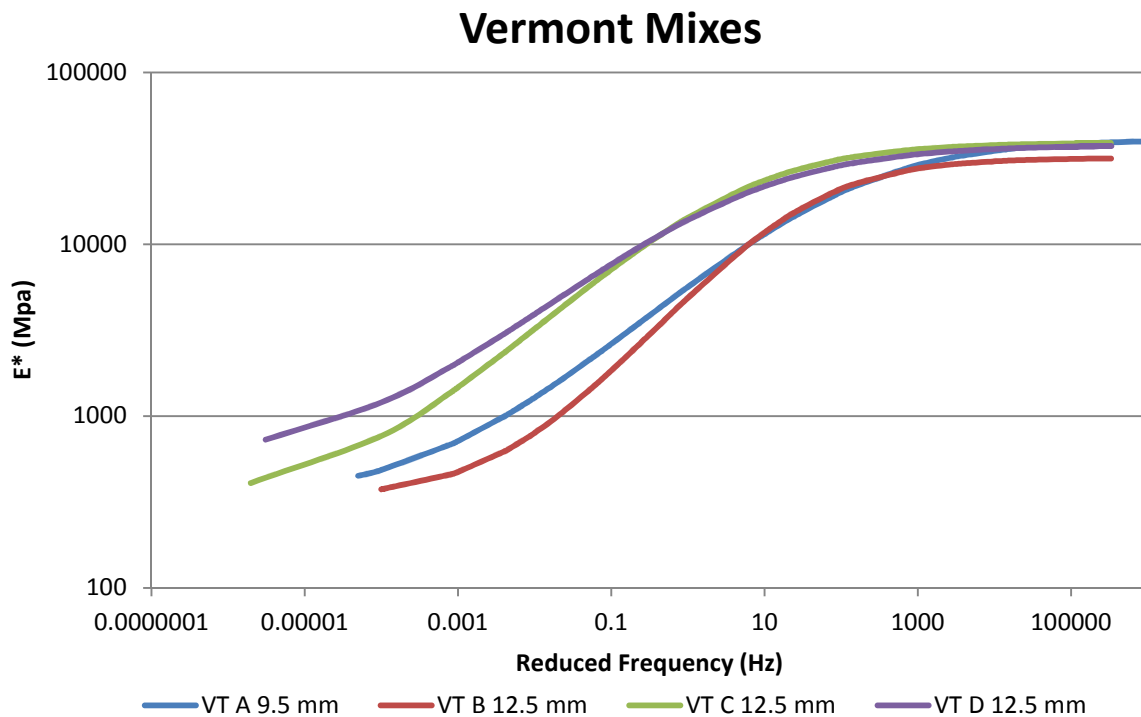


**Figure 5: Master Curves for Vermont Mixes**

## 5.2 Comparison of Laboratory and Plant Produced Mixes

In order to determine if there are any significant differences between laboratory mixed specimens and plant produced mix, specimens were fabricated in the laboratory using both methods of mixing materials. Plant mixed specimens were compacted from mix obtained by each state from paving jobs in progress at the time of material collection. Plant mixed material was not aged. However, lab mix was prepared according to job mix formulas and material obtained from each state agency. The lab mixes were aged in accordance the AASHTO R30. Paired samples of lab and plant mixed specimens were fabricated and tested in the UTM-25. Figure 6 contains comparison graphs of master curves for plant vs lab mixed materials for the representative mixes from each state. Also included in the graphs are the upper and lower error limits of the mean. The mean was calculated by averaging the lab mixes and plant mixed curves. Furthermore, the upper and lower error limits (shown using dashed lines) are based on the reported  $\pm 13.1\%$  accuracy (based on the number of replicates (2) and LVDTs (3) per sample per AASHTO TP 62-7). Analysis of paired plant vs lab mixes indicates some differences in  $|E^*|$  values. However, not all states can consider their lab mixed specimens to be the same as their plant mixed specimens. For Maine, the plant vs lab plot shows the entire master curves for those mixes fall outside the allowable mean error (dashed lines). Therefore, the plant and lab mixed specimens cannot be considered essentially the same mixture. For Vermont and New Hampshire the lab vs plant master curves fall within or on the error limits for the procedure. Therefore, these states can consider the plant and lab mixed specimens to be analogous. For the Rhode Island curves, the upper temperatures are within the allowable error while the lower temperatures tested fall outside the allowable error. Further testing may be necessary to determine if lab mixed samples are equivalent to plant mixed samples.

This comparison could not demonstrate that the  $|E^*|$  values obtained from corresponding mixes using plant produced material and lab produced material were identical for each state. However, limited number of lab vs plant replicates fabricated in this study prevents a statistically valid conclusion on whether plant produced material are representative of lab mixed material, and vice versa. Further research on this issue may be necessary to definitively determine the relationship between lab and plant mixed specimens.

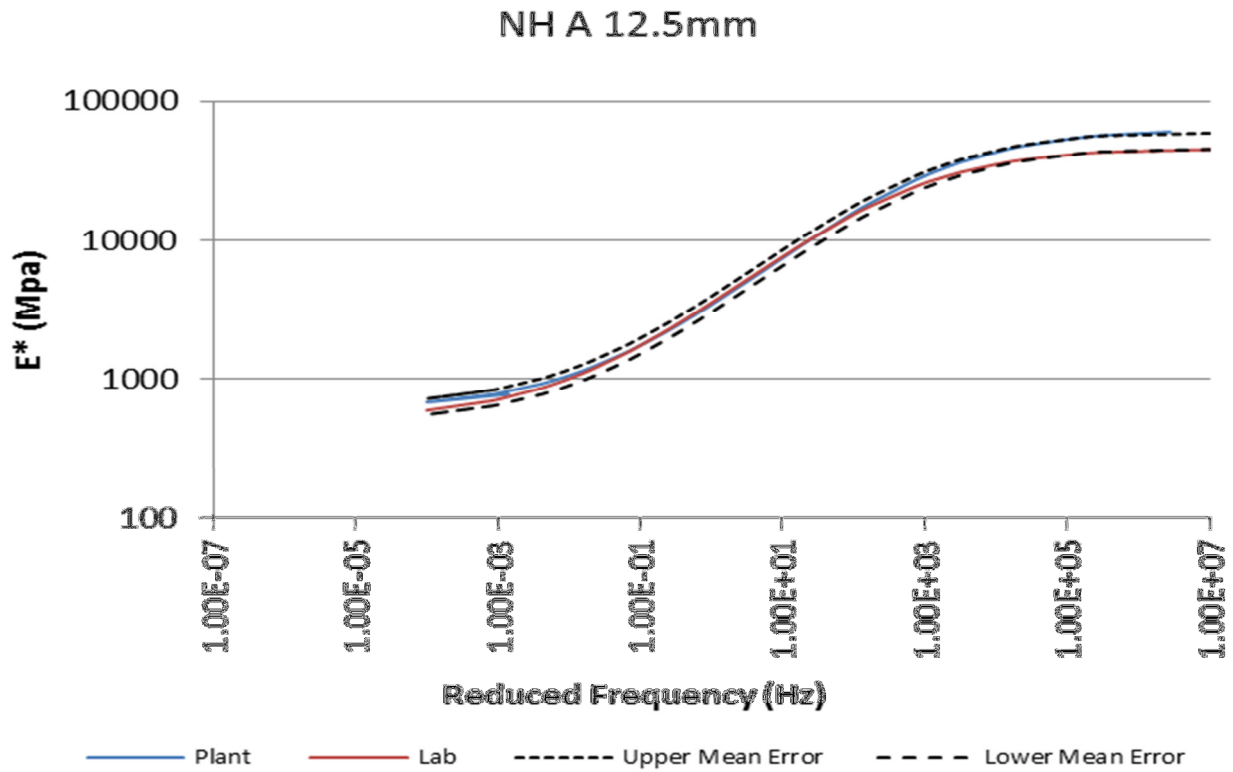
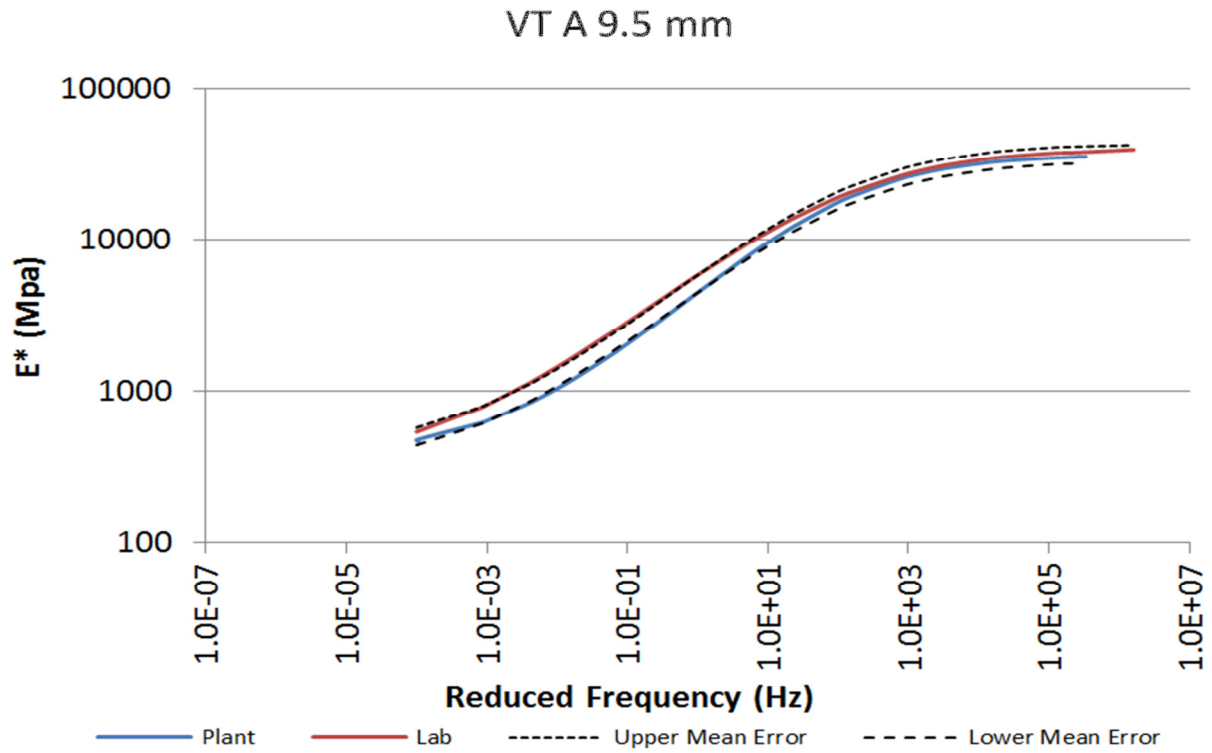
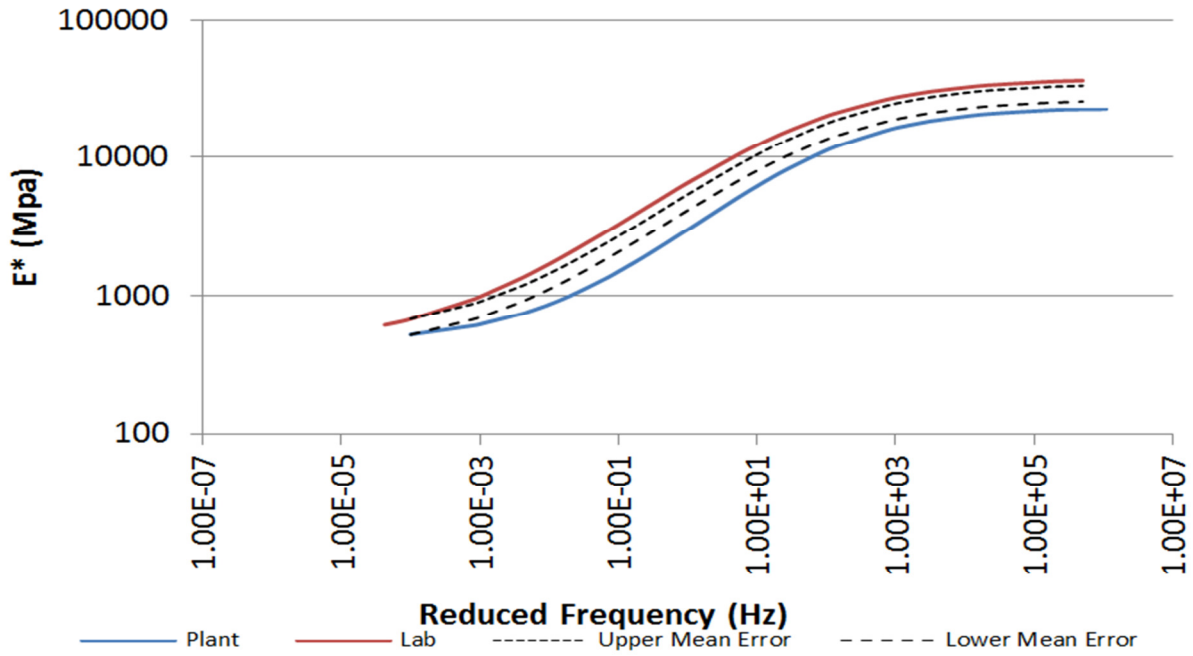


**Figure 6: Plant Vs Lab Master Curve Comparison**

### ME A 9.5 mm



### RI B 12.5mm

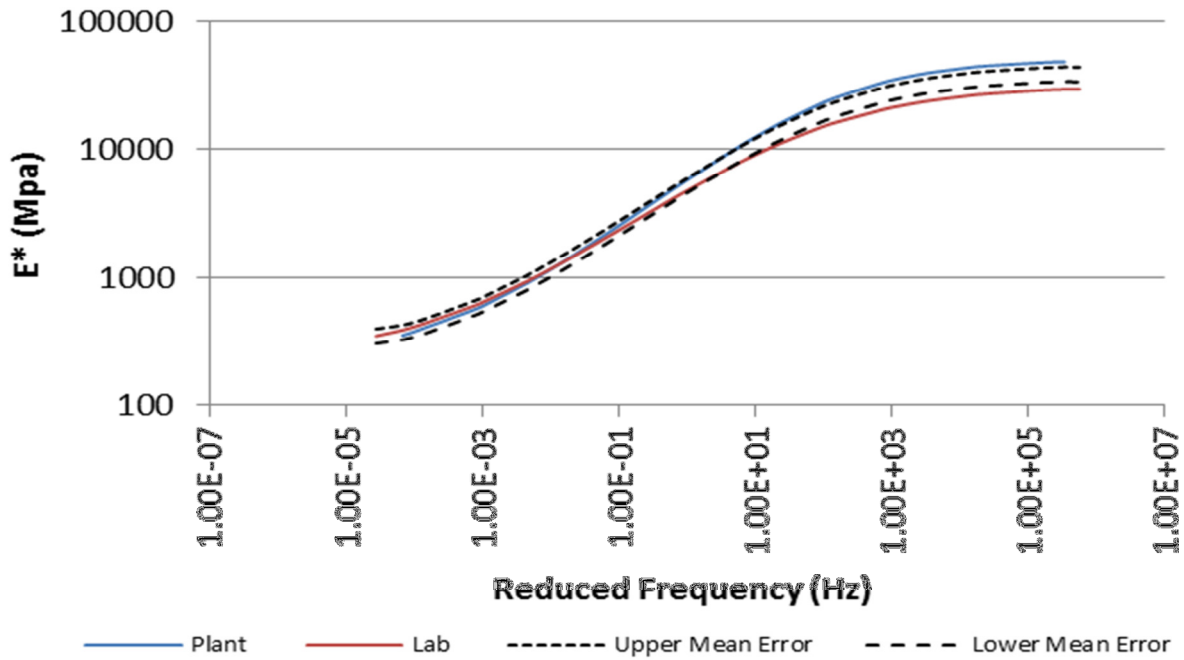


**Figure 6 (Cont.): Plant Vs Lab Master Curve Comparison**

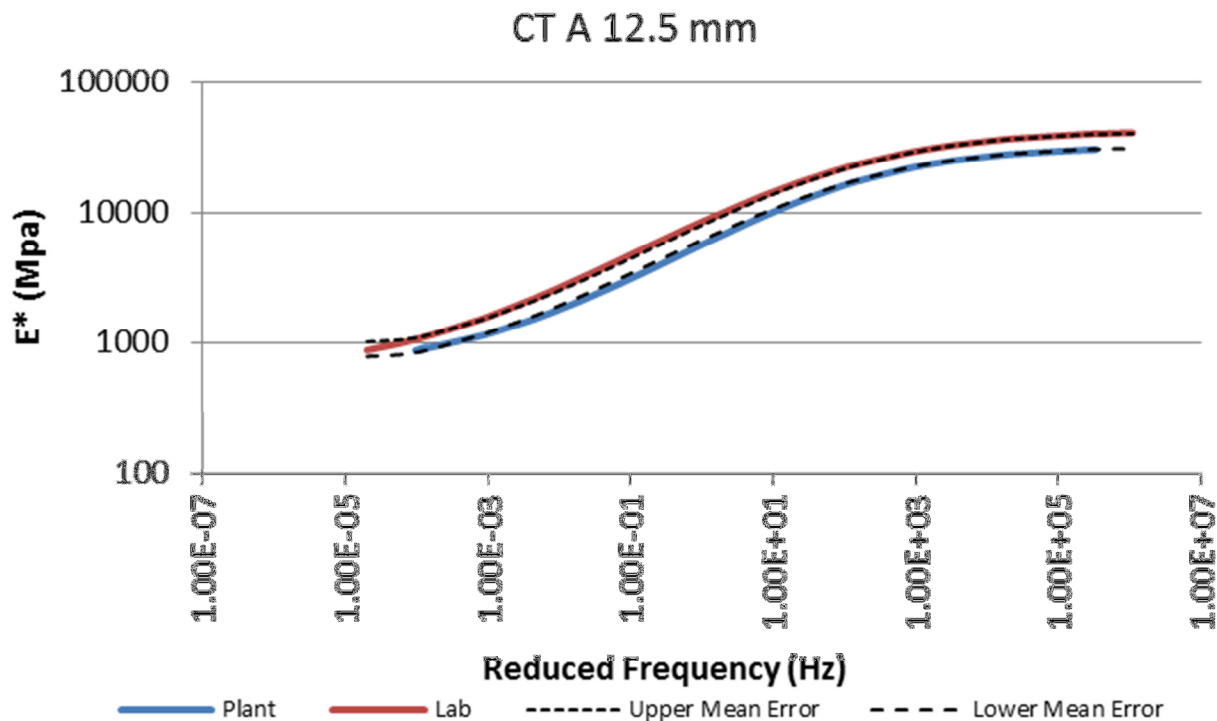


**Figure 6 (Cont.): Plant Vs Lab Master Curve Comparison**

### 5.3 Reduced Physical Modulus Testing

In an effort to simplify testing requirements and expensive testing machinery, Bonaquist and Christensen (2005) developed an alternative procedure eliminating the high and low temperature from dynamic modulus testing procedure. The high and low ends of the modulus curve were then predicted using the maximum and minimum modulus using the Hirsh model. Bonaquist and Christensen (2005) claimed that the current testing required substantial effort, with significant overlap in measured data which is not needed when numerical shifting methods are used to generate a master curve. Their alternative testing sequence requires testing at only three temperatures between 40°F and 115°F (4.4°C and 46.1°C) and four rates of loading between 0.01 and 10 Hz. This is in contrast to the 5 temperatures and 6 frequencies of the standard procedure outlined in Table 2. Bennett et. al., (2009) compared the accuracy and precision of the two testing protocols on variety of testing equipment. However, three of the seven laboratories used in their study did not have the capability to measure at 14F (-10C). In addition the  $E^*$

results at 14°F showed the highest variance and the 130°F produced the second highest degree of variation among the five test temperatures. The higher variance for the low and high temperatures was attributed to the accuracy of laboratory testing equipment at those temperatures. Then the reduced versus full testing curves were used in the MEPDS having all other factors identical. It was found that there were minimal changes in rutting prediction and a difference of approximately 35 ft/mi for the longitudinal cracking. Overall, Bennett et. al., (2009) concluded that the high and low test temperatures could be dropped from physical testing and could be predicted using a method similar to Bonaquist and Christensen (2005).

To investigate the impacts of a reduced testing procedure with that specified in AASHTO TP62-07, the test specimens were tested at the full temperature range and then the low and high temperatures were removed from the dataset. The resulting master curve plots can be found in Appendix B. On a state-by-state comparison it is easy to notice significant differences in the reduced testing plots and the full testing plots. The most notable change can be seen in the Vermont plots where the reduced testing procedure effective caused all the mixes to merge into a similar master curve. The same trend can be seen in the Connecticut mixes where the master curves become more homogenous. This reduction in curve variation between mixes may be correlated with the variation in  $|E^*|$  at the high and low testing temperatures noted by Bennett et. al, (2009). The impacts of the modified curves, via reduced testing, on the MEPDS predictions is beyond the scope of this project, but should be investigated further before a reduced testing protocol is used as input for the MEPDS in New England. The significant visual changes to the master curves, seen in Appendix B, indicates there are potential disadvantages to reducing the range of testing temperatures. Specimen fabrication was the most time consuming and difficult part of this data collection process. Therefore, if a facility has the ability to test the full range of temperatures and frequencies for each specimen they took the time to fabricate, then they should do so. The rest of this report uses the data collected from all temperature ranges as specified in AASHTO TP 62.

#### **5.4 Master Curve Predictions Using Mix and Binder Specifications**

The use of a predictive model to estimate dynamic modulus would eliminate the need to conduct expensive and labor intensive sample fabrication and mechanical testing. Based on models identified in the background section of the report, the necessary variables were collected to predict  $|E^*|$  without mechanical testing of specimens. These predictions were generated for the exact mix designs provided. In addition to the volumetric data and gradation data provided by each state, binder testing was also conducted to generate master curves for the binders used in each mix. These master curves were generated using a DSR. The following three models were used to predict  $|E^*|$  and generate a master curve for each state mix: Andrei-Witczak, Hirsch, and ODB. Three variations of the basic ODB model were considered. The first run was the fitted static modulus value, the second was run with default values suggested by ODB, the third run was conducted by fitting  $E_{inf\_mix}$  using Witczak model. The initial runs showed that the second variation provided the most robust predictions. Therefore, only this version of ODB model is compared with Andrei-Witczak and Hirsch models next. The MEPDS uses the Witczak model to predict the  $|E^*|$  of asphalt materials. Therefore, comparisons between the measured  $|E^*|$  values and the values predicted by the Witczak model are analogous to comparison between measured  $|E^*|$  values and the  $|E^*|$  that would be predicted and used in MEPDS.

Figure 7 is an example mix (CT A 12.5 mm) showing the measured  $|E^*|$  values compared to the predicted  $|E^*|$  values using each of the models discussed earlier. The predicted  $|E^*|$  values from each established model are on the Y-axis. The X-axis contains the corresponding measured  $|E^*|$  value. If models were absolutely correct, all the data points should follow a 45 degree line labeled “Measured” (Line of Equality, LOE) as indicated by the blue line in the figure. However, the equations for predicating  $|E^*|$  are 100% accurate for these mixes. Therefore any deviation from this blue line indicates a region or area where the model is inaccurate. From this figure it appears that at lower temperatures (higher  $|E^*|$ ) the predictive models under estimate  $|E^*|$ . In most cases,  $|E^*|$  is under predicted by half (100% error). Conversely at higher Temperatures (lower  $|E^*|$ ) the models fall slightly above and below the measured  $|E^*|$  values. This graph is most commonly plotted on a log-log axis (Figure 8). Figure 8 reinforces the findings in Figure 7.

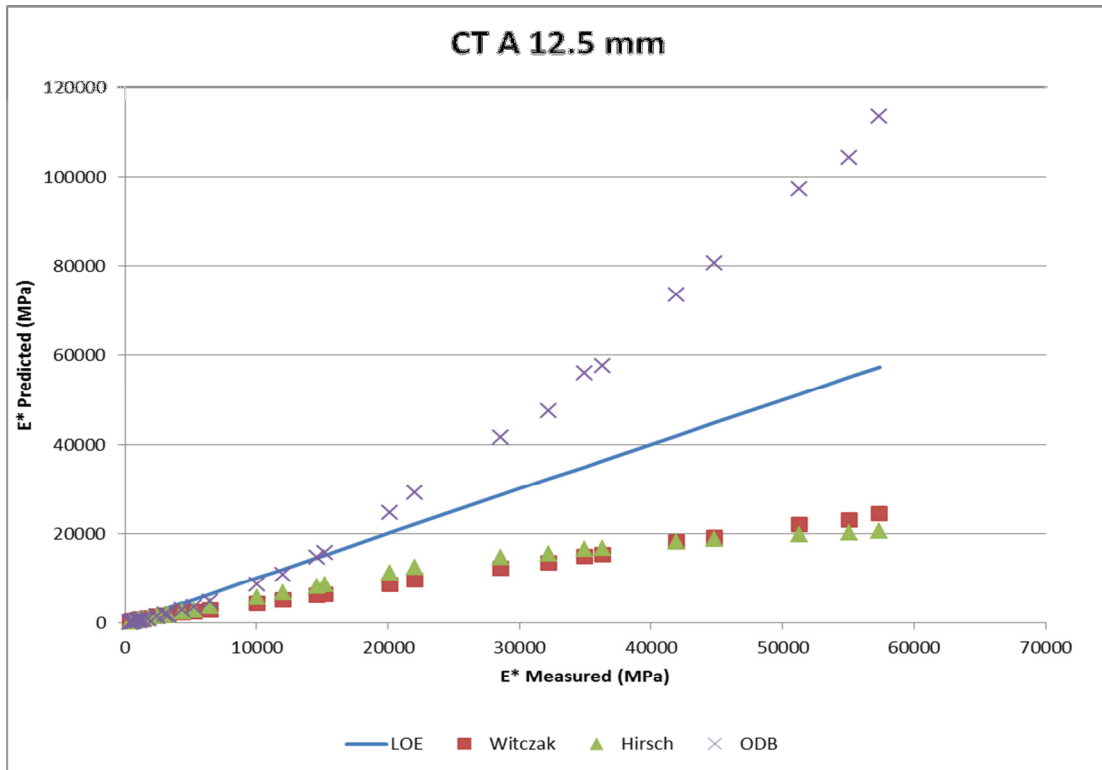


**Figure 7: Predicted Vs Tested |E\*| Values (MPa) (linear scale) (CT A 12.5 mm)**

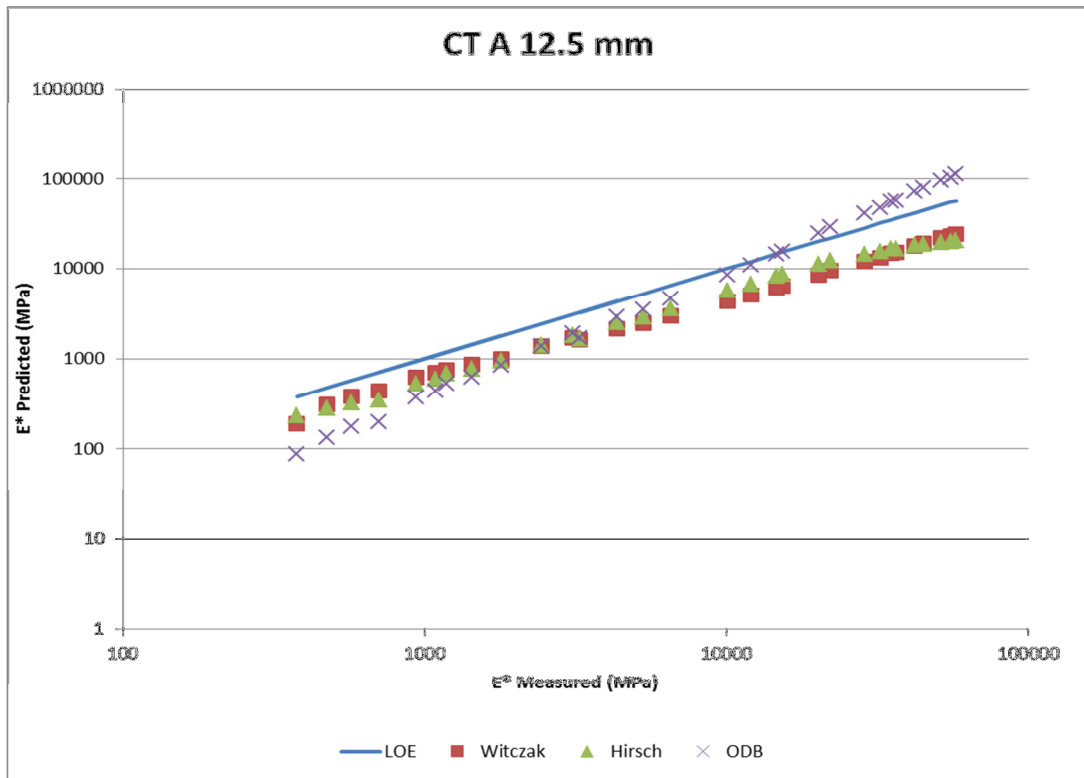


**Figure 8: Log-Log Plot of Predicted Vs Tested |E\*| Values (MPa) (CT A 12.5 mm)**

The log–log plot indicates what appears to be a relative constant offset of the predicted vs measured  $|E^*|$  values. For the CT A 12.5 mm mix it appears the equations are predicting  $|E^*|$  values that are approximately half that of the measured  $|E^*|$ .

Table 3 contains the scale factor for each predictive model and each mix for each state. The state and mix specific scale factors were determined by using the solver function in Excel to minimize the percent error between measured and modeled  $|E^*|$  values. For the mix specific scale factor, the percent error for each mix was minimized. For the state specific scale factor, a single factor was derived which resulted in an average mean absolute error for the all mixes tested. The mean and standard deviation of the scale factors on the Witczak and Hirsch models indicate that a scale factor of approximately 2 and 1.7 respectively are common for mixes in the New England Region. For the ODB models a standard deviation nearly half the mean 0.36 Vs 0.87 indicates less confidence in a global mean scale factor for this model. Furthermore the ODB model has a much higher percent error than the other two models (Table 4).

**Table 3: Model Scale Factors**

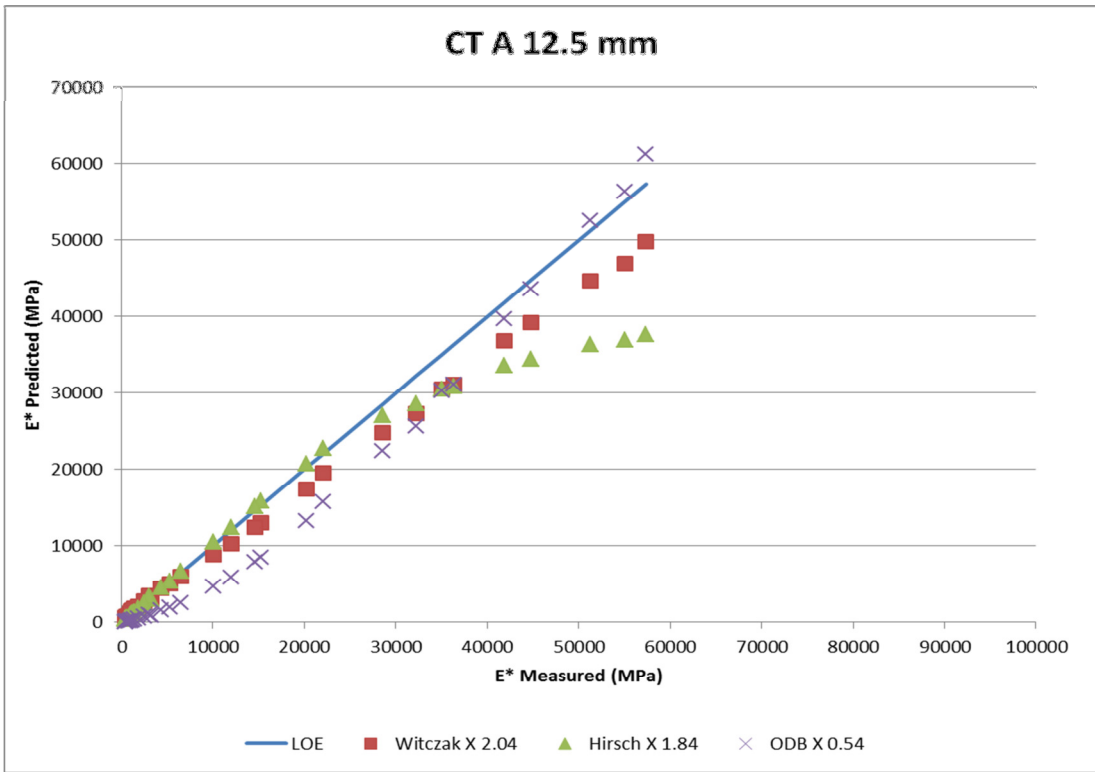
Mix	Mix and State Specific Scale Factor			State Specific Scale Factor		
	Witczak	Hirsch	ODB	Witczak	Hirsch	ODB
CT A 12.5 mm	2.04	1.84	0.54	1.61	1.45	0.48
CT B 12.5 mm	1.61	1.62	0.53			
CT C 12.5 mm	1.28	1.15	0.45			
CT D 12.5 mm	1.89	1.69	0.56			
VT A 9.5 mm	1.82	1.54	0.62	1.86	1.58	0.70
VT B 12.5 mm	1.77	1.54	1.15			
VT C 12.5 mm	1.93	1.76	0.67			
VT D 12.5 mm	2.08	1.54	0.52			
NH A 12.5 mm	2.40	2.05	0.75	2.01	1.74	0.76
NH B 9.5 mm	1.84	1.59	0.70			
NH C 19 mm	2.55	2.12	1.04			
NH D 25 mm	2.01	1.76	0.79			
ME A 9.5 mm	2.17	2.09	1.35	2.12	2.04	1.48
ME C 12.5 mm	2.58	2.61	1.89			
ME D 19 mm	1.59	1.43	1.11			
RI A M CL-1	1.98	1.83	0.91	2.02	1.86	0.97
RI B 12.5 mm	2.11	1.95	1.02			
RI C M CL-1	2.00	1.91	1.01			
Average	1.99	1.78	0.87	1.93	1.74	0.88
Max	2.58	2.61	1.89	2.12	2.04	1.48
Min	1.28	1.15	0.45	1.61	1.45	0.48
Stdev	0.32	0.32	0.36	0.20	0.23	0.38

Table 4 presents the mean absolute percent error before and after the use of the mix specific scale factor and a state specific scale factors presented in Table 3. In general the application of the scale factor significantly reduced the percent error between the measured and predicted  $|E^*|$  values. The Witczak model showed the greatest reduction in percent error, 51% to 19%. While this is still not within the 13.1% error associated with number of replicates number and LVDTs used as quoted in AASHTO TP 62, it is a significant improvement over the 51% mean error associated with the non-scaled Witczak model. Furthermore, table 4 indicates there are minimal gains in accuracy when applying a mix specific scale factor.

**Table 4: Percent Error Reduction Pre and Post Scale Factors Applied**

Mix	Mean Percent Error Before Scale Factor Applied			Mean Percent Error After Mix Specific Scale Factor Applied			Mean Percent Error After State Specific Factor Applied		
	Witczak	Hirsch	ODB	Witczak	Hirsch	ODB	Witczak	Hirsch	ODB
CT A 12.5 mm	50	16	123	16	15	54	21	15	54
CT B 12.5 mm	41	16	112	24	15	55	24	15	55
CT C 12.5 mm	27	20	96	15	18	57	22	18	58
CT D 12.5 mm	47	20	117	13	18	59	16	18	59
VT A 9.5 mm	55	21	95	28	15	50	28	15	50
VT B 12.5 mm	48	19	42	17	15	41	18	15	53
VT C 12.5 mm	50	14	107	11	14	44	12	15	45
VT D 12.5 mm	53	29	115	19	14	47	20	16	49
NH A 12.5 mm	58	18	102	17	15	57	18	15	59
NH B 9.5 mm	47	18	85	8	15	57	10	15	57
NH C 19 mm	60	19	71	19	15	54	23	15	55
NH D 25 mm	60	17	84	27	14	57	27	14	57
ME A 9.5 mm	57	13	54	12	13	44	12	13	44
ME C 12.5 mm	63	13	49	15	13	44	21	13	44
ME D 19 mm	39	15	47	20	13	44	32	14	45
RI A M CL-1	52	14	73	25	13	47	25	13	47
RI B 12.5 mm	52	14	64	14	13	44	15	13	44
RI C M CL-1	59	20	75	33	19	55	33	19	56
Average	51	18	84	19	15	51	21	15	52
Max	63	29	123	33	19	59	33	19	59
Min	27	13	42	8	13	41	10	13	44
Stand. Dev.	9	4	26	7	2	6	7	2	6

Figures 9 and 10 contain a plot of predicted  $|E^*|$  values that have been multiplied by a scale factor increase the accuracy in predicted  $|E^*|$ . These plots indicate that by scaling the predicted  $|E^*|$  the accuracy of the  $|E^*|$  values predicted by each equation has greatly improved. Comparison graphs for each mix can be found in Appendix C.



**Figure 9: Scaled Predicted Vs Tested  $|E^*|$  Values (MPa) (linear scale) (CT A 12.5 mm)**

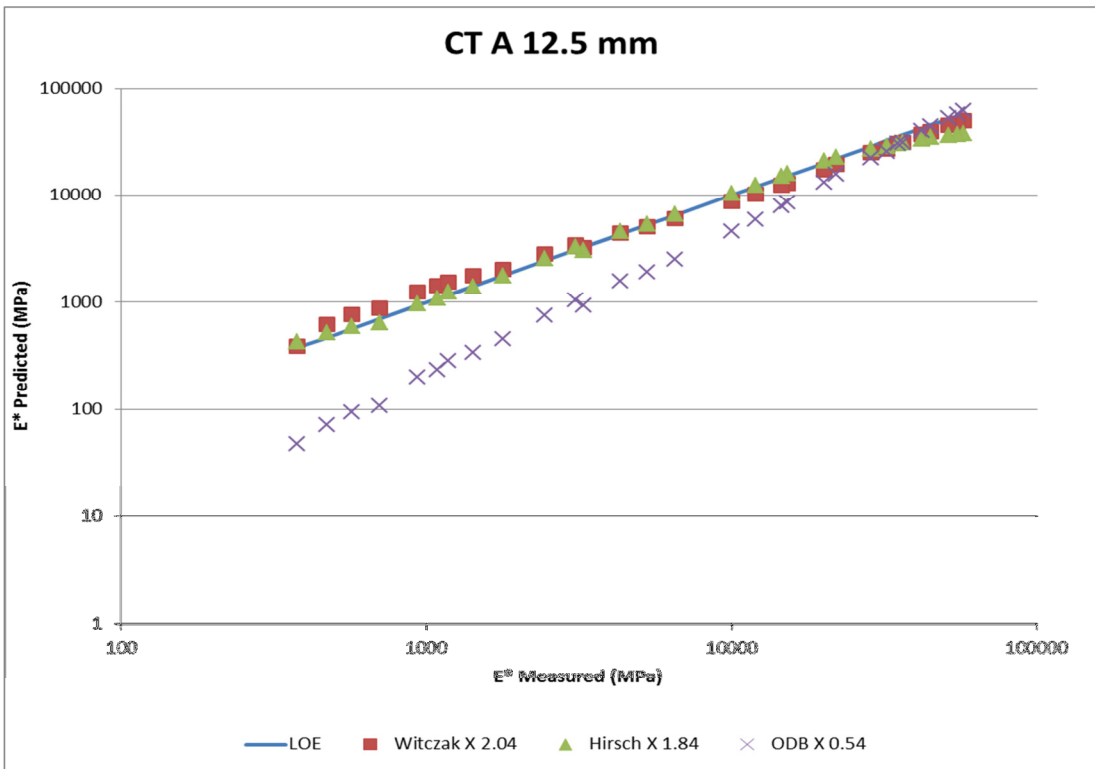


**Figure 10: Log-Log Plot of Scaled Predicted Vs Tested  $|E^*|$  Values (MPa) (CT A 12.5 mm)**

## 6.0 CONCLUSIONS

The primary objective of this research is to test commonly used HMA mixtures throughout New England to determine their respective dynamic modulus master curves. The resulting plots of master curves and dynamic modulus values can be found in Appendix A.

### 6.1 New England Mix Conclusions

Various asphalt concrete mix designs across New England were analyzed to determine if there is a significant difference between dynamic modulus values for materials from throughout the region. Based on the resulting master curves and scale factor analysis presented above it is apparent that mixes in the New England region are not dramatically different from one another in terms of dynamic modulus. The results of the scaling factor analysis indicate that each state has a scale factor of approximately 2 for the Witczak equations used in the MEPDS (Table 3). Furthermore, Figure 11 displays a representative 12.5 mm, 64-28, 15% RAP (Note: RI was excluded since the RI 12.5 mm mix was 76-28 and 0% RAP) mixes for the participating New England states. While the master curves shown converge on the high and low end, there are differences from state to state in the magnitude and inflection points of the curve. The Vermont mix falls considerably below the Maine mix, by up to 15,000 MPa at a reduced frequency of 800 Hz. The Connecticut and New Hampshire mixes have a nearly identical shape with only a slight shift in magnitude. Based on the reported accuracy of the test each curve could be shifted as much as 13.1%. This shift would result in the Connecticut, Maine and New Hampshire mixes overlapping throughout the majority of the curve. Therefore, of the mixes tested from each state it can be assumed that there is little to no variation in master curves for the mixes in New England region. However, further testing on more mixes may be necessary to confirm this finding. One should also keep in mind, that the ultimate comparison between  $|E^*|$  curves should be based upon pavement performance predictions from the MEPDS. It is likely that even if two curves appear to be visually different, they may result in similar MEPDS predictions.

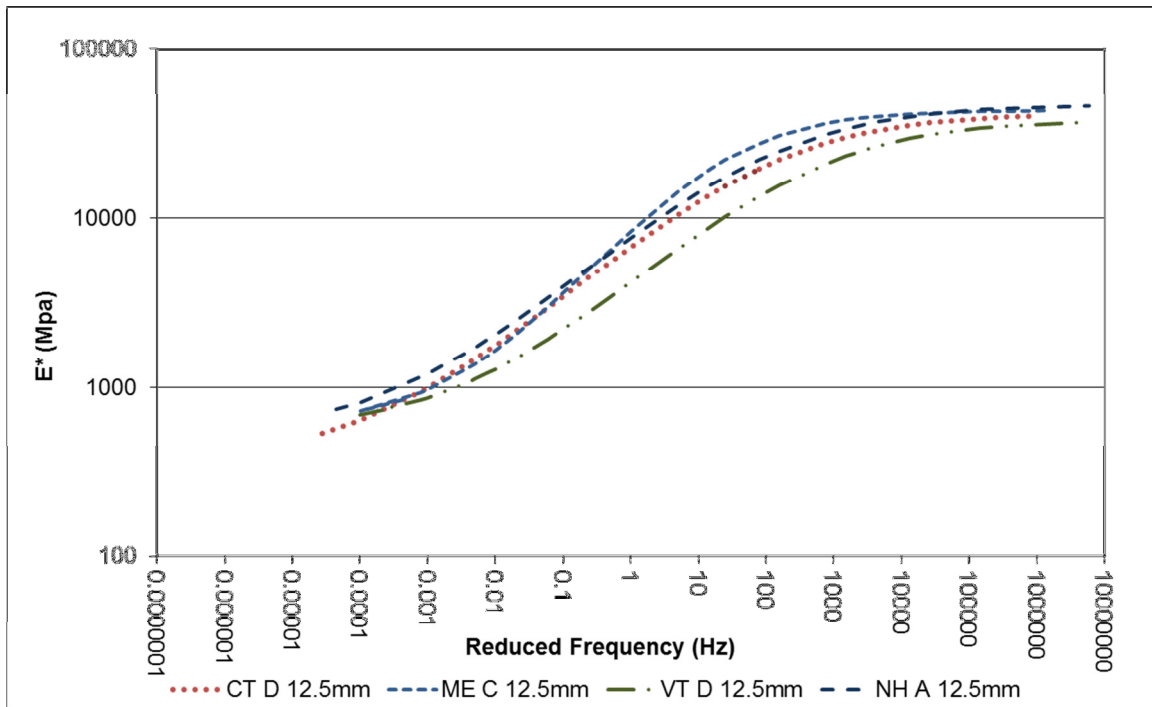


**Figure 11: State-by-State Comparison of 12.5mm, 64-28, 15% RAP Mixes**

## 6.2 Lab vs Plant Conclusions

Analysis of master curves generated from plant produced mix and lab produced mix, of identical mix designs and properties (Figure 6) indicates there are not dramatic differences between the two material mixing methods for testing. However, there were differences observed for the Maine mixes that exceeded the stated accuracy of the AASHTO test method TP 62-18. Further testing should be conducted with a larger number of replicate pairs (plant vs lab prepared) to determine, statistically, on a state by state basis if specimen fabrication method has a significant impact on master curve development.

## 6.3 Reduced Testing Curve Comparison

A comparison of a full scale testing and a reduced testing procedure, as proposed by Bonaquist and Christensen (2005), was conducted to determine if New England states could reduce the number of temperatures and frequencies used to generate an  $|E^*|$  master curve. While there is literature that suggests the impacts of reduced testing is minimal on the predictions of the MEPDS, this analysis indicates there is a significant visual change in master curve shape when reducing the testing protocol. Assessing these impacts on the results of the MEPDS is beyond the scope of this project but should be examined to determine if New England states should adopt the reduced testing protocol. Considering the time and effort alone that is required to fabricate the minimum of 2 samples for testing, this study recommends to conduct a full testing suite on each specimen as recommended by AASHTO TP62-07 (5 temperatures and 6 frequencies at each temperature). Therefore, if a facility has the equipment capable to test the full range of temperatures, the extra few hours required to allow the specimen to reach thermal equilibrium is well justified and eliminates any dispute when developing  $|E^*|$  master curves.

#### **6.4 Measured vs Predicted $|E^*|$ Comparison**

Comparison of measured  $|E^*|$  values and those that would be predicted by the MEPDS (via the basic Witczak equation) indicates that the predicted  $|E^*|$  curves would be approximately half of the  $|E^*|$  values that were actually obtained via mechanical testing (Table 3). Furthermore, this study also presents each state with a scaling factor for Hirsch, Witczak and ODB models (Table 3). These scaling factors will allow each state to predict the dynamic modulus values for each of their mixes based on mix design, thus reducing the need for expensive and labor intensive mechanical testing. Therefore, if the MEPDS is to be used in New England for pavement design, modifications need to be made to the dynamic modulus predictive equation and/or performance models need to be calibrated for local conditions.

## 7.0 REFERENCES

AASHTO TP 62, 2010. Standard Method of Test for Determining Dynamic Modulus of Hot-Mix Asphalt Concrete Mixtures, AASHTO Designation TP 62. AASHTO Provisional Standards, AASHTO, Washington DC.

AASHTO, 1986. American Association of State Highway and Transportation Officials (AASHTO). AASHTO Guide for Design of Pavement Structures. Washington, DC.

AASHTO, 1993. American Association of State Highway and Transportation Officials (AASHTO). AASHTO Guide for Design of Pavement Structures. Washington, DC.

Andrei, D., M. W. Witzak, and M. W. Mirza. *Development of Revised Predictive Model for the Dynamic (Complex) Modulus of Asphalt Mixtures*. NCHRP 1-37A Inter Team Report, University of Maryland, 1999.

Bari, J., and M.W. Witzak. 2005. Evaluation of the Effect of Lime Modification on the Dynamic Modulus Stiffness of Hot-Mix Asphalt, In *Transportation Research Record: Journal of the Transportation Research Board*, Transportation Research Board of the National Academies, Washington, D.C., pp. 10-19.

Bennett, Thomas and Stacy Goad Williams. 2009. Precision of AASHTO TP62-07 for Use in Mechanistic–Empirical Pavement Design Guide for Flexible Pavements. *Transportation Research Record: Journal of the Transportation Research Board*, No. 2127, Transportation Research Board of the National Academies, Washington, D.C., 2009, pp. 115–126.

Birgisson, B., G. Sholar, and R. Roque. 2005. Evaluation of Predicted Dynamic Modulus for Florida Mixtures. CD-ROM. Transportation Research Record of the National Academies, Washington, D.C.

Bonaquist, R., and D. W. Christensen. 2005. Practical Procedure for Developing Dynamic Modulus Master Curves for Pavement Structural Design. In *Transportation Research Record: Journal of the Transportation Research Board*, Transportation Research Board of the National Academies, Washington, D.C., pp.208-217.

Bonaquist, R.F., D. W. Christensen, and W. Stump. 2003. *Simple Performance Tester for Superpave Mix Design: First-Article Development and Evaluation*. NCHRP Report 513. Transportation Research Board of the National Academies, Washington, D.C.

Christensen, D.W., T. Pellinen, and R. F. Bonaquist. 2003. Hirsch Model for Estimating the Modulus of Asphalt Concrete. *Journal of Association of Asphalt Paving Technologist*, Vol. 72, pp. 97-121.

Daniel, J. S. and A. Lachance. 2005. Mechanistic and Volumetric Properties of Asphalt Mixtures with RAP. In *Transportation Research Record: Journal of the Transportation Research Board*, Transportation Research Board of National Academies, Washington, D.C.

Di Benedetto, H., F. Olard, C. Sauzeat, and B. Delaporte. 2004. Linear Viscoelastic Behavior of Bituminous Materials: from binders to mixes. *Road Materials and Pavement Design*, Vol. 6.

Dongré, R., L. Myer, J. D' Angelo, C. Paugh, and J. Gudimettla. 2005. Field Evaluation of Witczak and Hirsch Models for Predicting Dynamic Modulus of Hot-Mix Asphalt. *Journal of the Association of Asphalt Paving Technologists*, Vol. 74, pp. 381-442.

Fonseca, O. A., and M. W. Witczak. 1996. A Prediction Methodology for the Dynamic Modulus of In-Placed Aged Asphalt Mixtures. *Journal of the Association of Asphalt Paving Technologists*, Vol. 65., pp. 532-572.

Gordon, G.V., and M. T. Shaw. 1994. *Computer Programs for Rheologists*. Hanser/Gardner Publ.

Hirsh, T. J. 1961. *The Effect of Elastic moduli on the Cement Paste Matrix and Aggregate on Modulus of Elasticity of Concrete*. Ph. D. Thesis. Agricultural and Mechanical College of Texas, College Station Texas.

Huang, B., B. K. Egan, W. R. Kingery, Z. Zhang, and G. Zuo. 2004. Laboratory Study of Fatigue Characteristics of HMA Surface Mixtures Containing RAP. CD-ROM. Transportation Research Board of National Academies, Washington, D.C.

Li, X., M. O. Marasteanu, R. C. Williams, and T. R. Clyne. 2008. Effect of Reclaimed Asphalt Pavement (Proportion and Type) and Binder Grade on Asphalt Mixtures, In *Transportation Research Record: Journal of the Transportation Research Board*, Transportation Research Board of National Academies, Washington, D.C., pp. 90-97.

Masad, E., H. Bahia. 2002. Effects of Loading Configuration and Material Properties on Non-Linear Response of Asphalt Mixtures. *Journal of the Association of Asphalt Paving Technologists*, Vol. 71, pp. 535-558.

MATLAB (R2009b). 2009. The Math Works Inc.

NCHRP 1-37A, 2004. Development of the 2002 Guide for Design of New and Rehabilitated Pavement Structures: Phase II,. National Cooperative Highway Research Program, NCHRP Project 1-37A, Washington, DC.

Olard, F., and H. Di Benedetto. 2003. General "2S2P1D" Model and Relation Between the Linear Viscoelastic Behaviors of Bituminous Binders and Mixes. *Road Materials and Pavement Design*, Vol. 4.

Pellinen, T., A. Zofka, M. Marasteanu, and N. Funk. 2007. Asphalt Mixture Stiffness Predictive Models. *Journal of the Association of Asphalt Paving Technologists*, Vol. 76, pp 575-625.

Rowe, G. M., G. Baumgardner and M. J. Sharrock. 2008. A Generalized Logistic Function to

Describe the Master Curve Stiffness Properties of Binder Mastics and Mixtures, 45<sup>th</sup> Petersen Asphalt Research Conference, University of Wyoming.

Rowe, G. M., S. Hakimzadeh, and P. Blankenship. 2009. Evaluation of Asphalt of  $|E^*|$  Test Using HMA Specimens with Varying Void Contents. In *Transportation Research Record: Journal of the Transportation Research Board*, Transportation Research Board of National Academies, Washington, D.C., pp. 164-172.

Seo, Y., O. El-Haggan, M. King, S.J. Lee, and Y.R. Kim. 2007. Air Void Models for the Dynamic Modulus, Fatigue Cracking, and Rutting of Asphalt Concrete. *Journal of Materials in Civil Engineering*, Vol. 19.

Shaw, M. T., and W. J. Macknight. 2005. *Introduction to Polymer Viscoelasticity, Third Edition*. John Wiley and Sons, Inc., New Jersey.

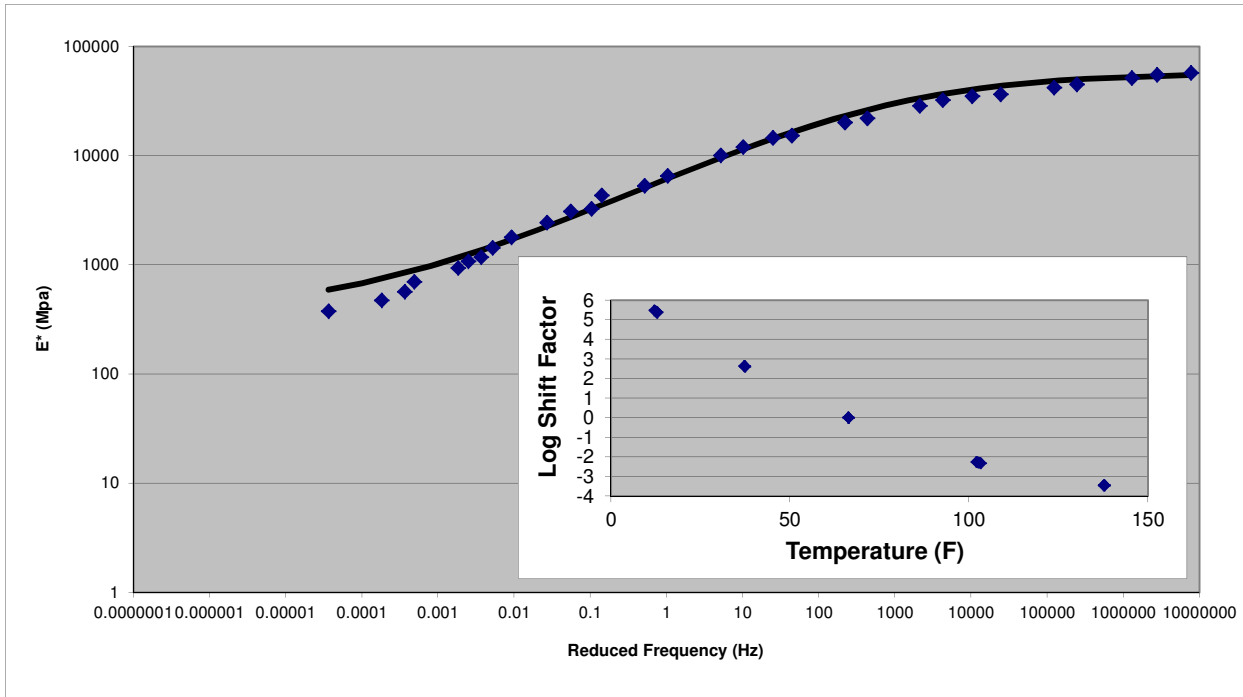
Shook, J.F., and B.F. Kallas. 1969. Factors Influencing Dynamic Modulus of Asphalt Concrete. *Journal of the Association of Asphalt Paving Technologists*, Vol. 38.

University of Maryland Superpave Support and Performance Management Team. 1998. *Development of Relationships Between Binder Viscosity and Stiffness*. FHWA Superpave Models Inter Team Technical Report, University of Maryland, May 1998.

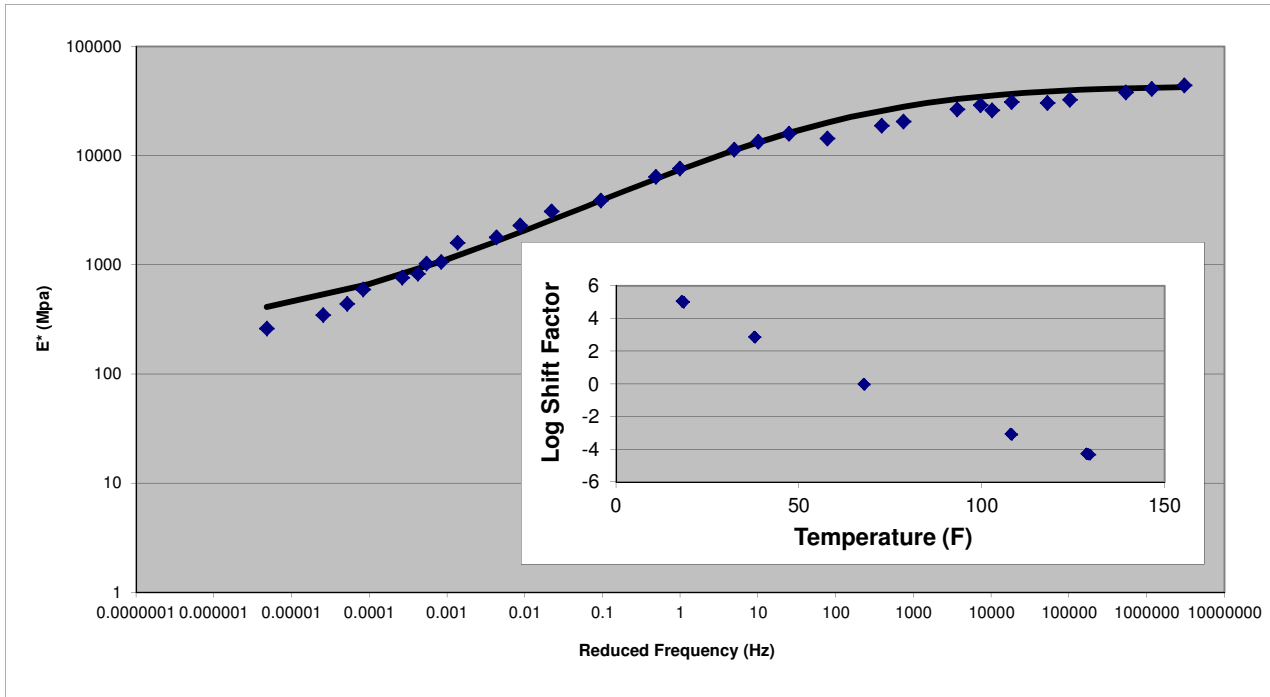
Witczak, M.W. 2005. *Simple Performance Tests: Summary of Recommended Methods and Database*. NCHRP Report 547. Transportation Research Board of the National Academies, Washington, D.C., 2005.

## **APPENDIX A: MIX AND STATE SPECIFIC MASTER CURVES**

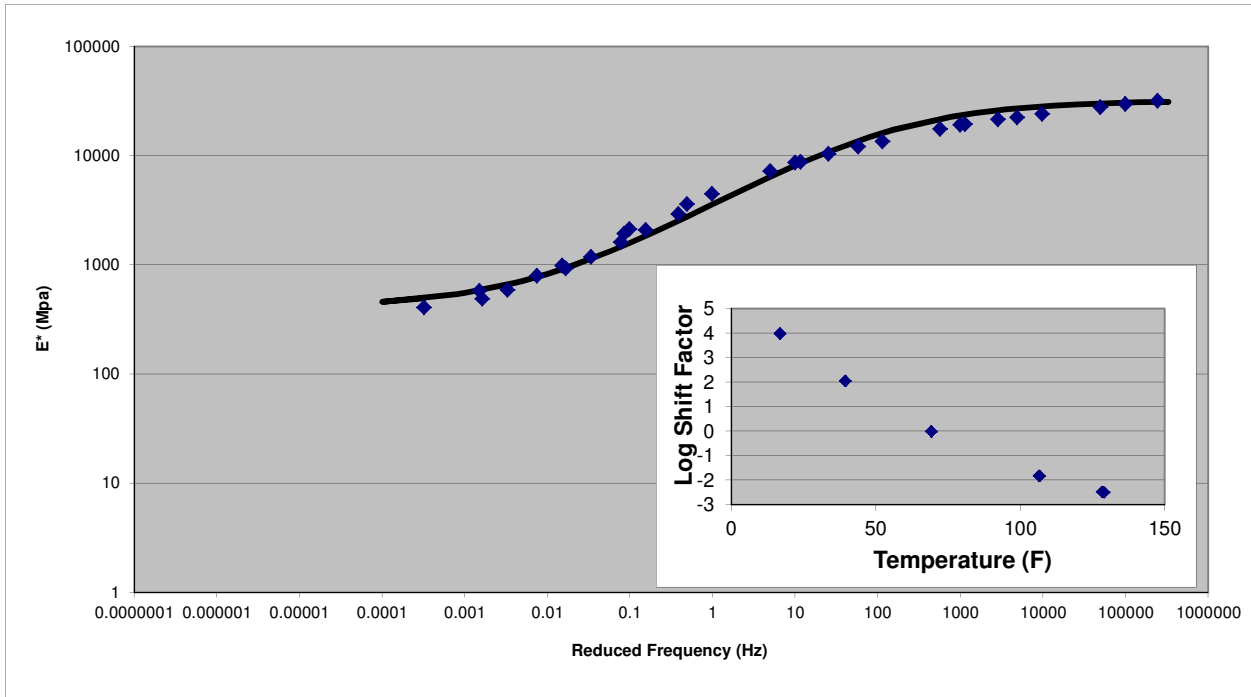
CT A 12.5 mm



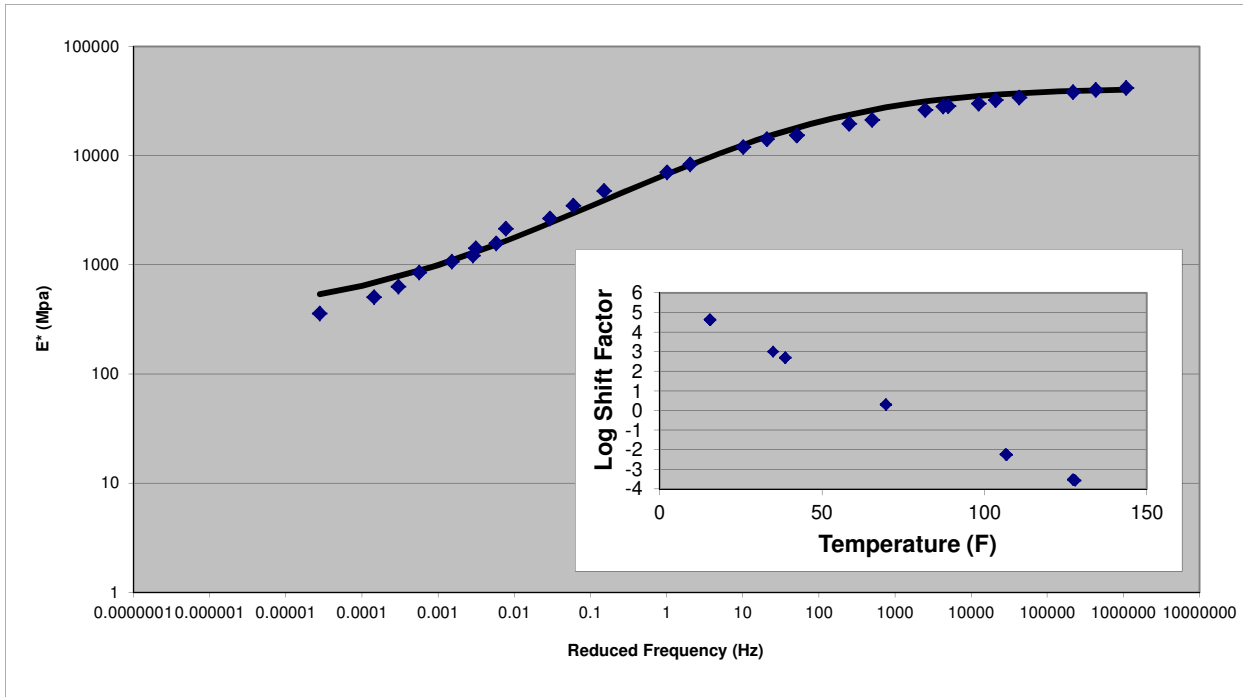
CT B 12.5 mm



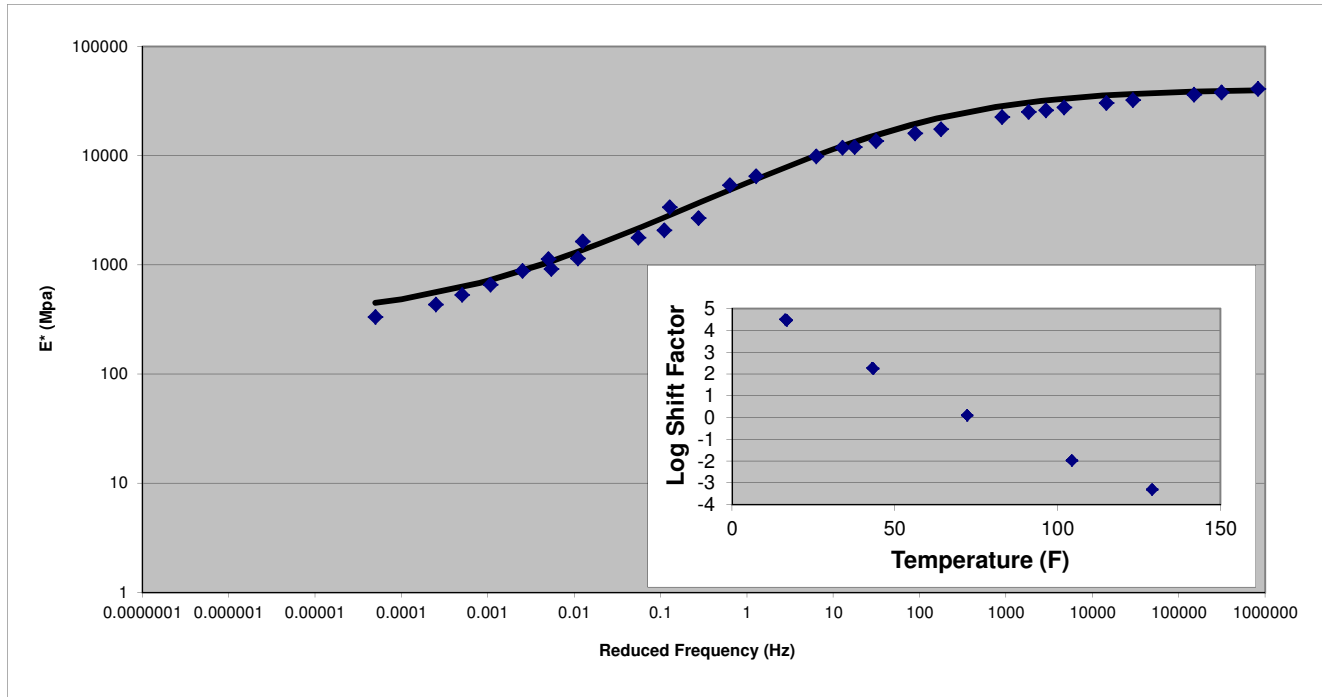
CT C 12.5 mm



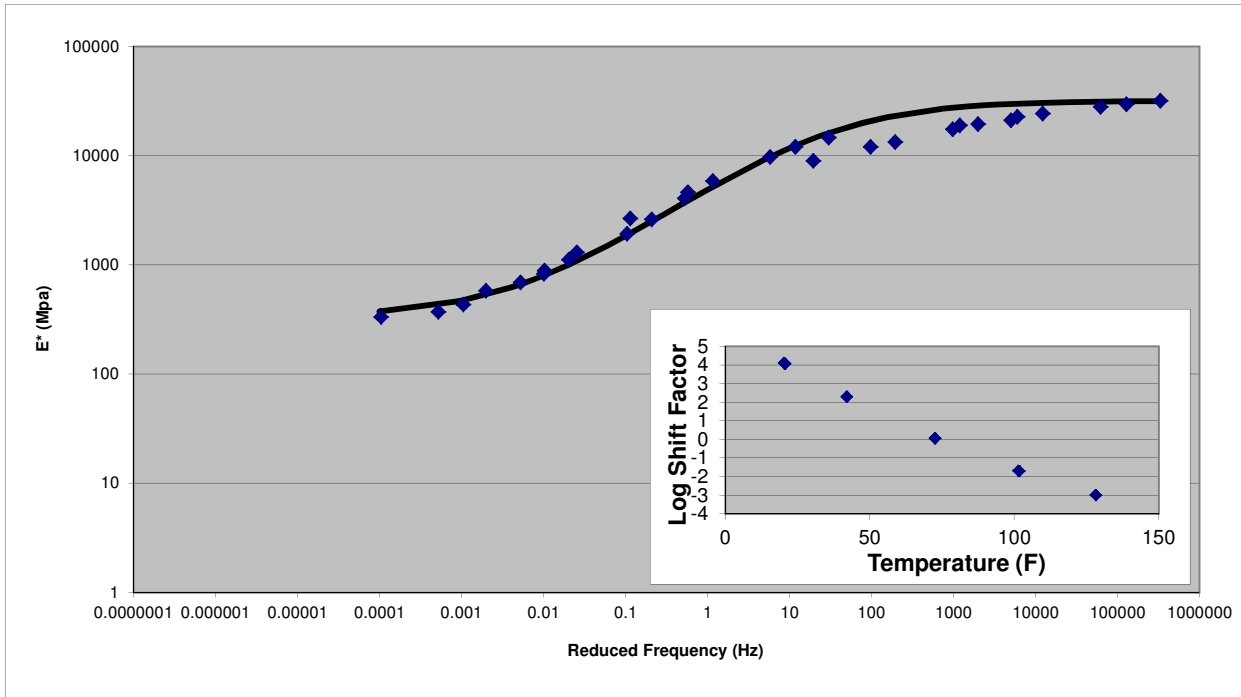
CT D 12.5 mm



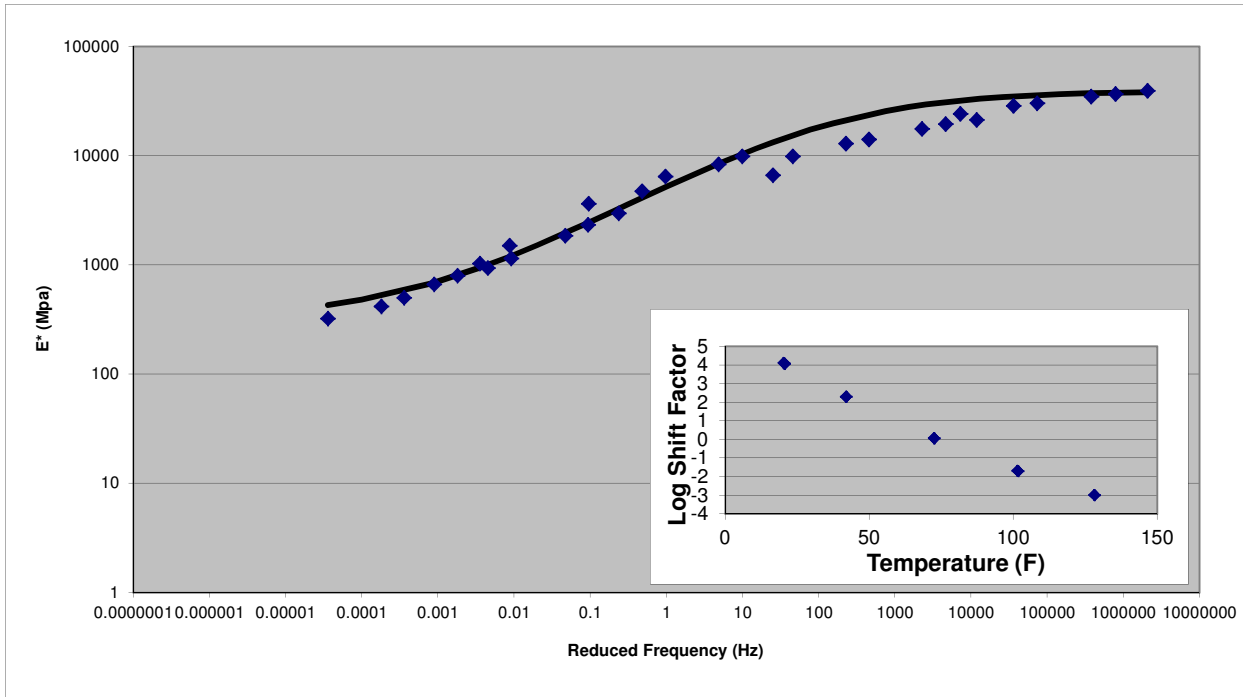
VT A 9.5 mm



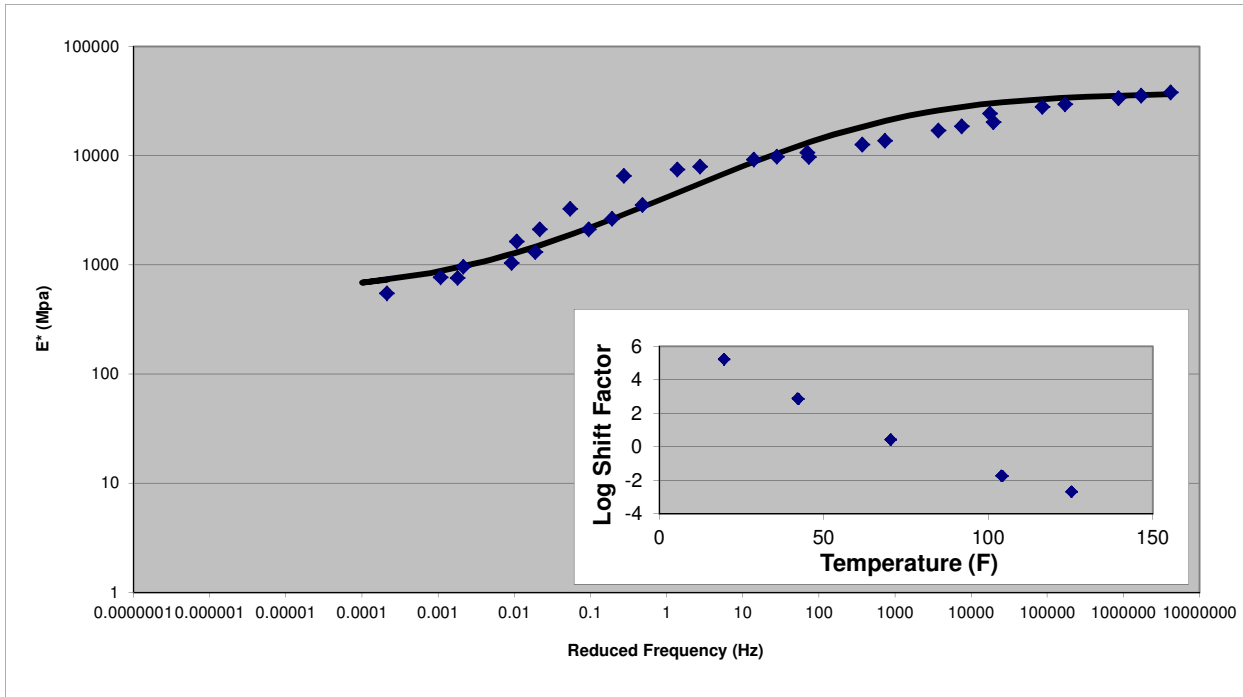
VT B 12.5 mm



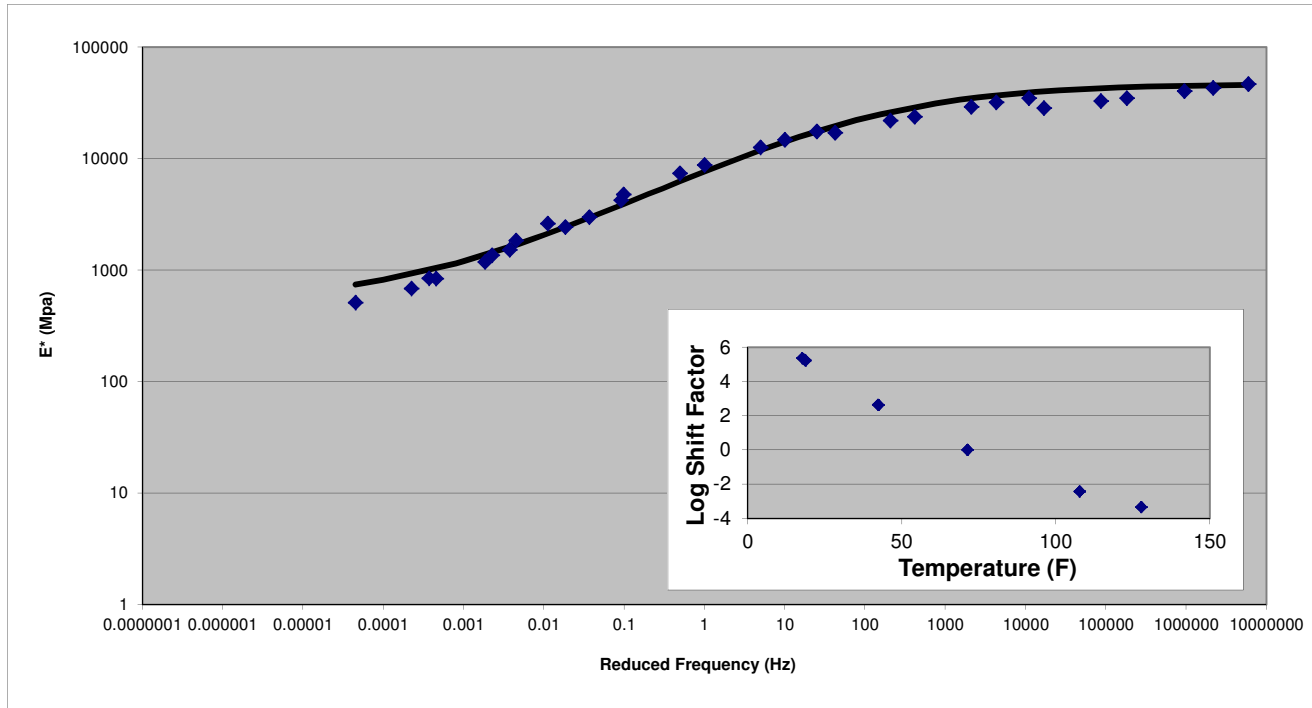
VT C 12.5 mm



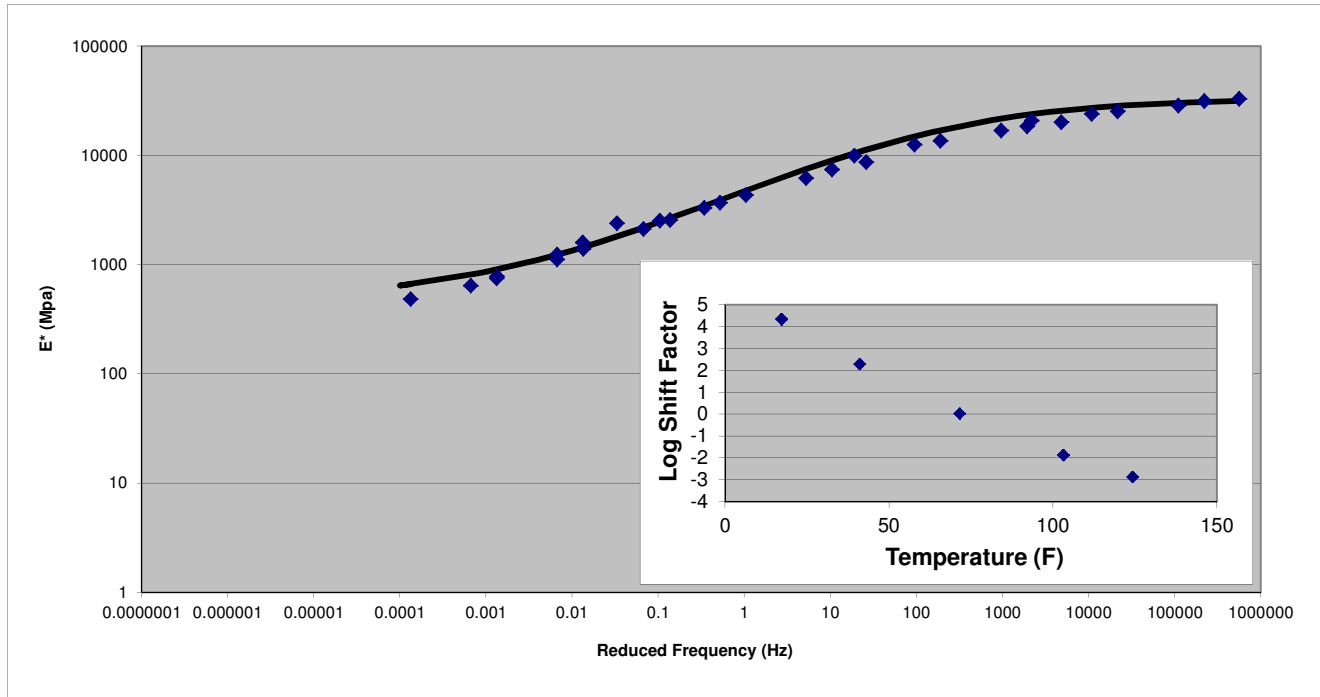
VT D 12.5 mm



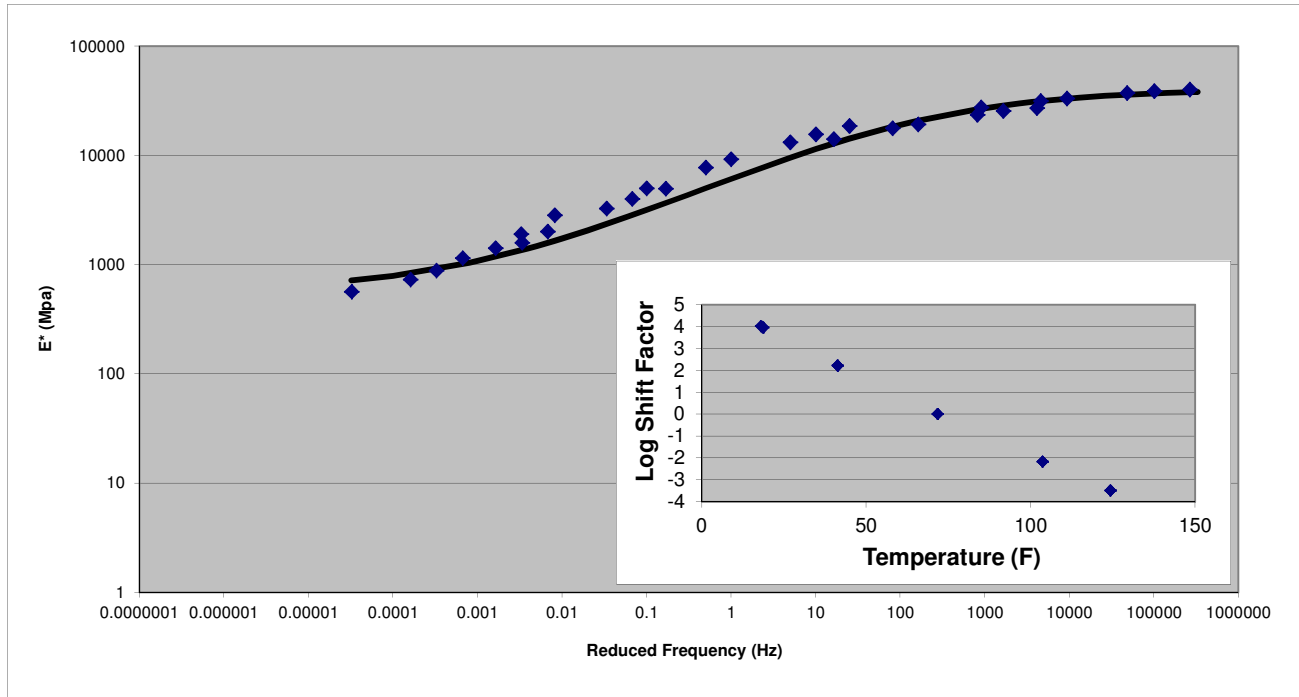
NH A 12.5 mm



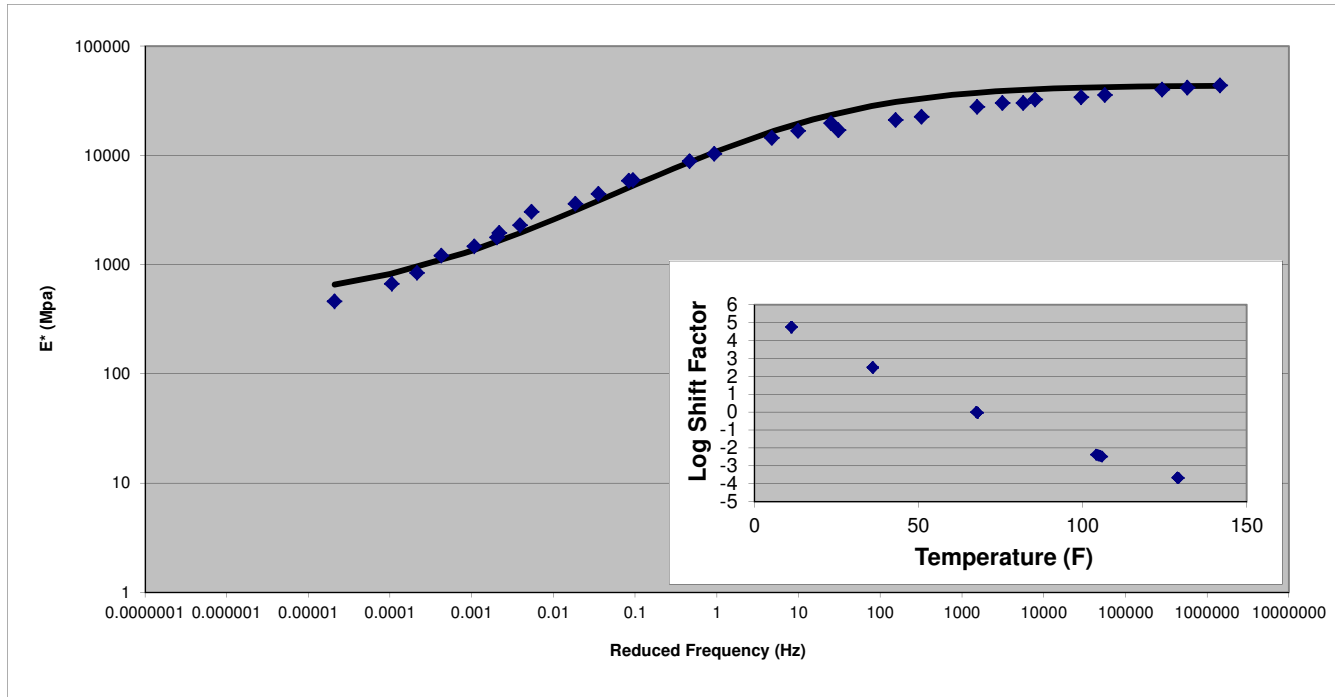
NH B 9.5 mm



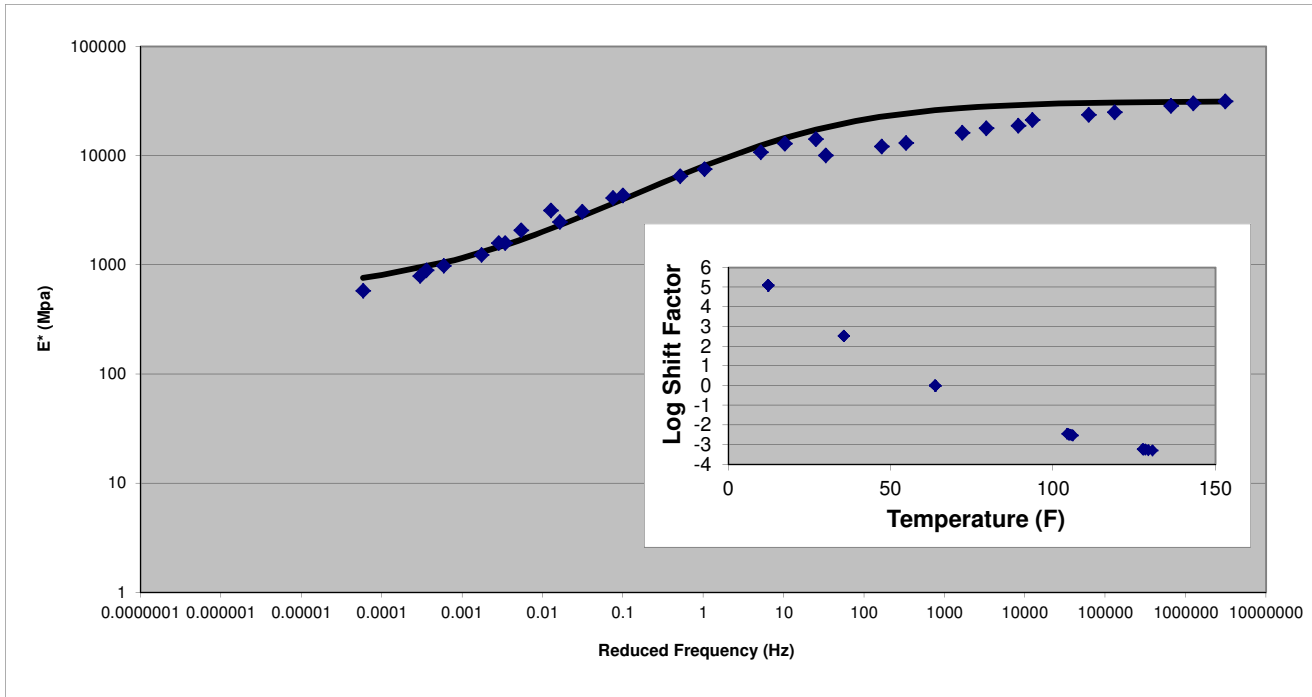
NH C 19 mm



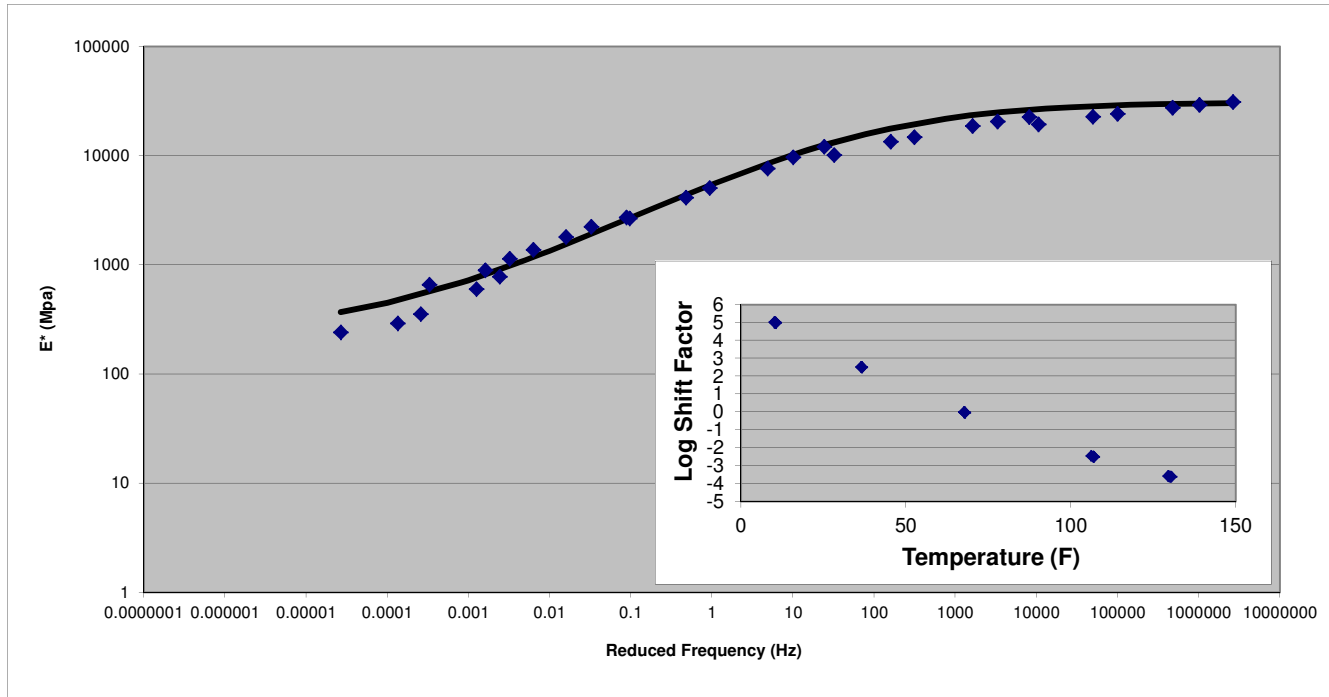
NH D 25 mm



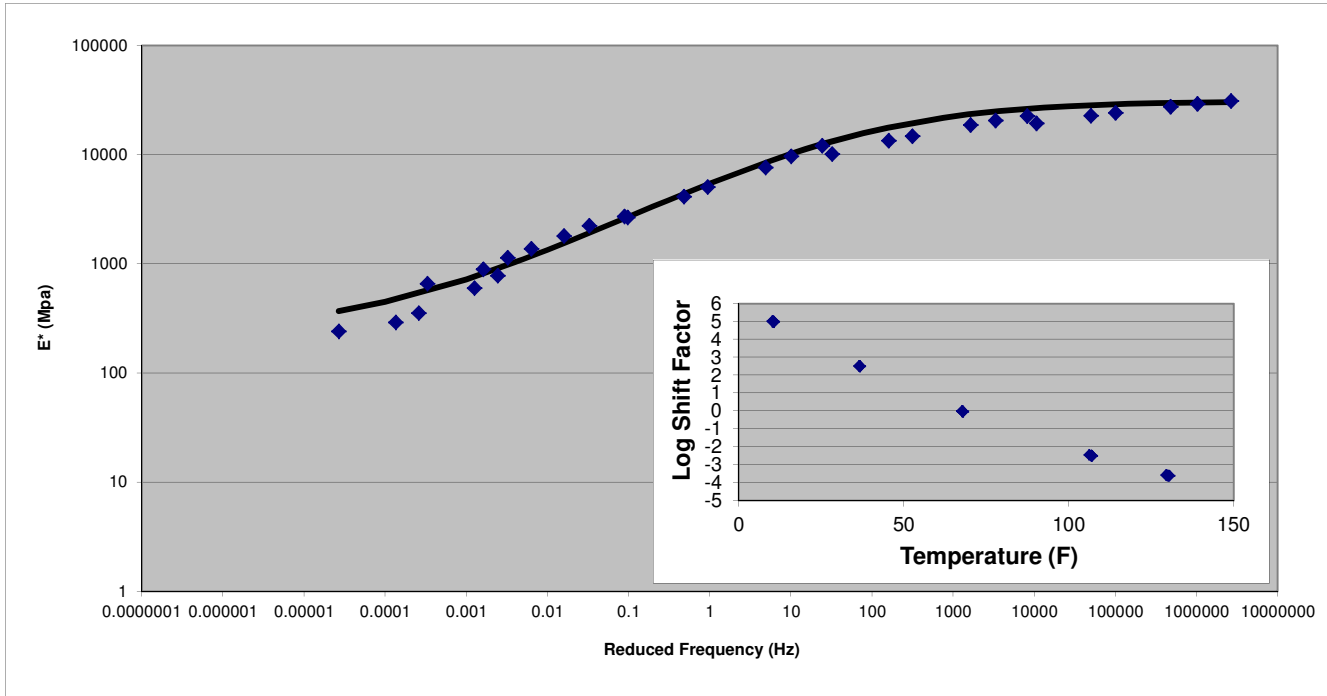
ME A 9.5 mm



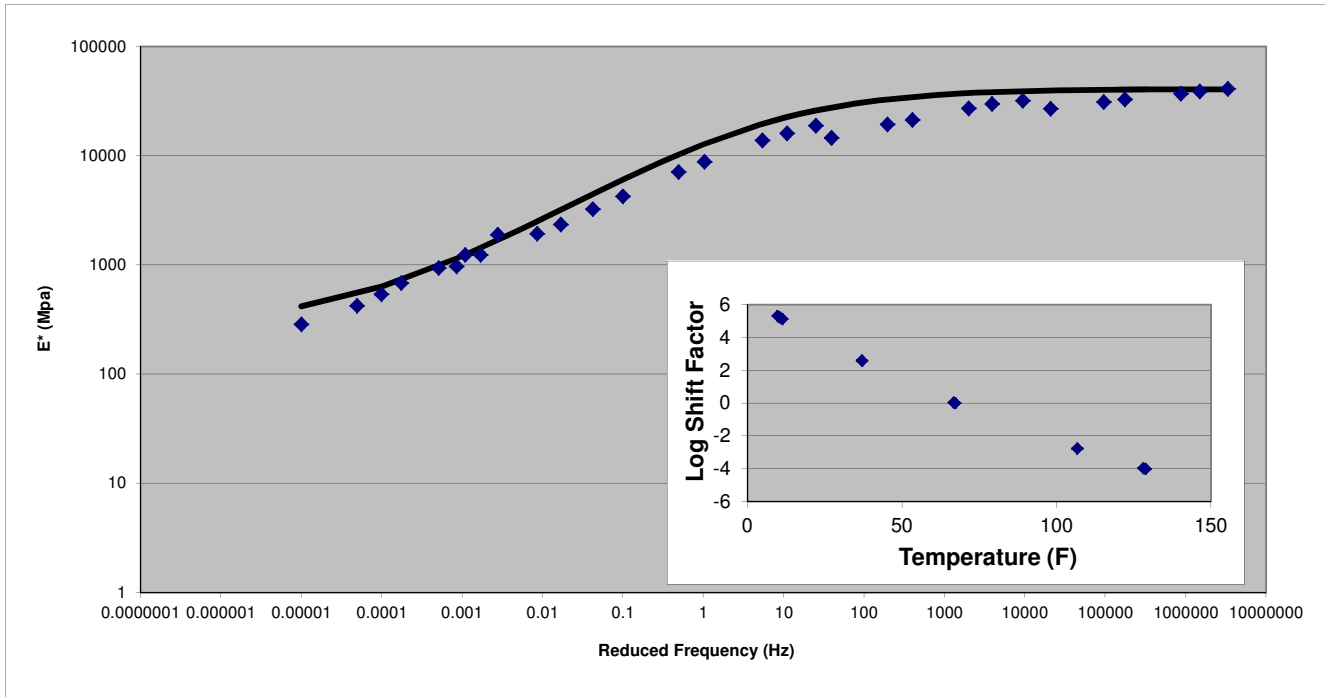
ME C 12.5 mm



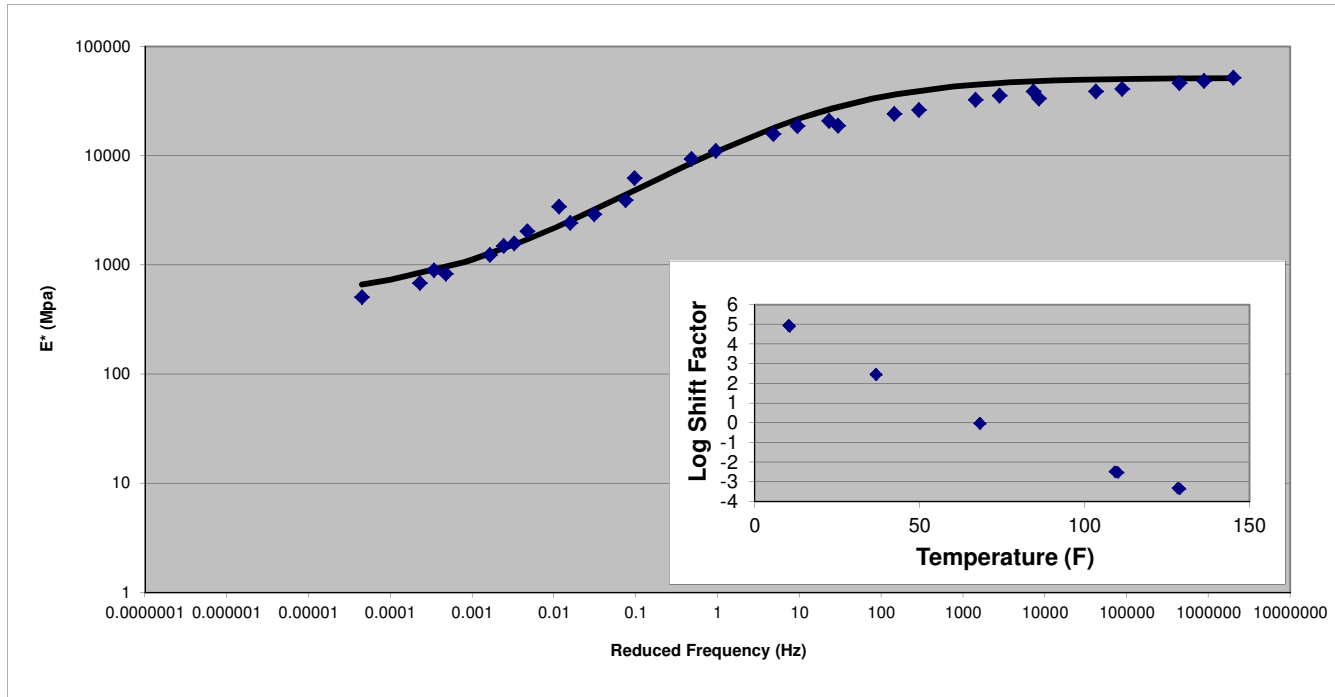
ME D 19 mm



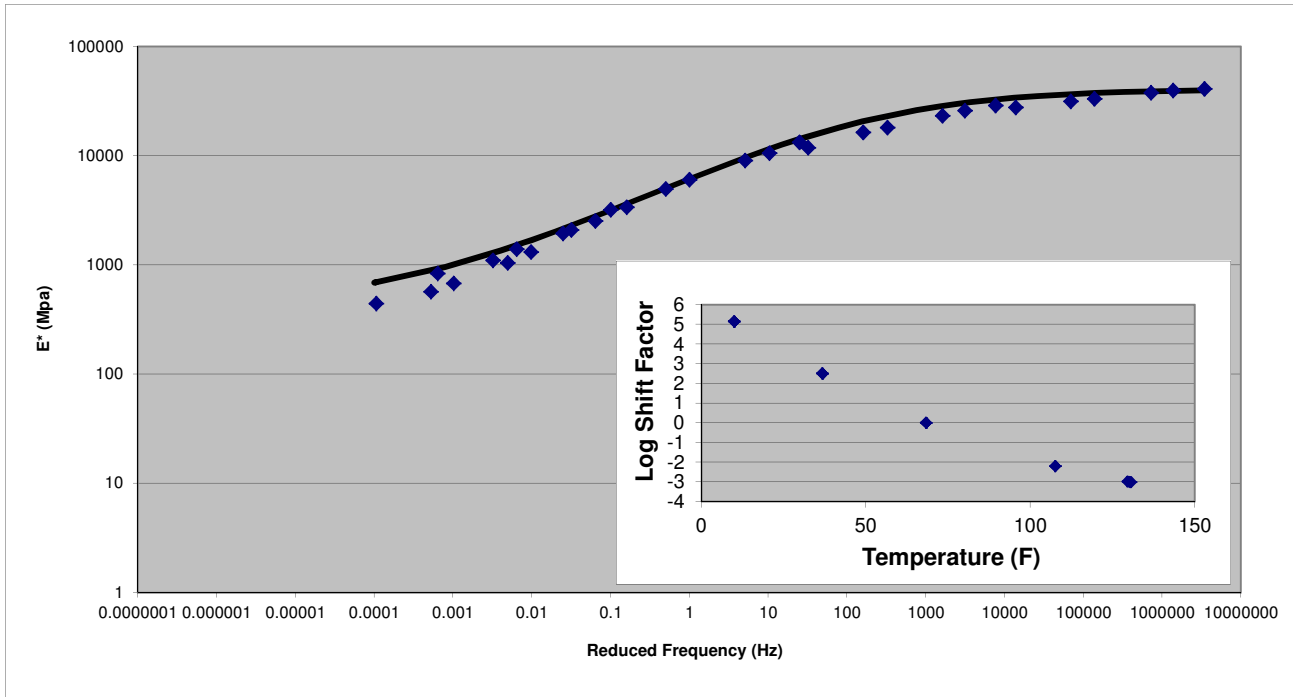
RI A M CL-1



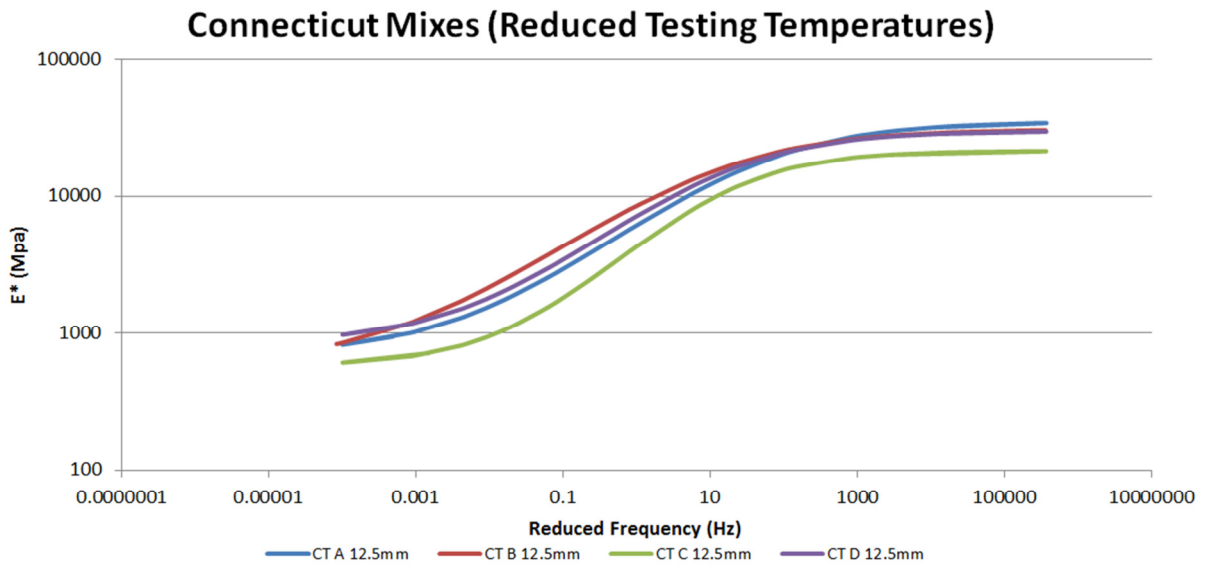
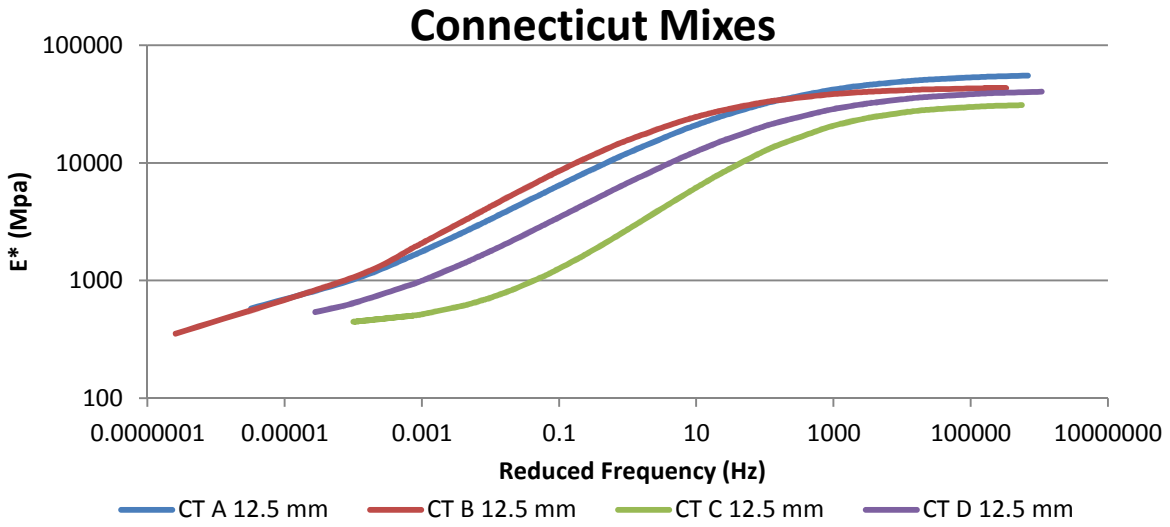
RI B 12.5 mm



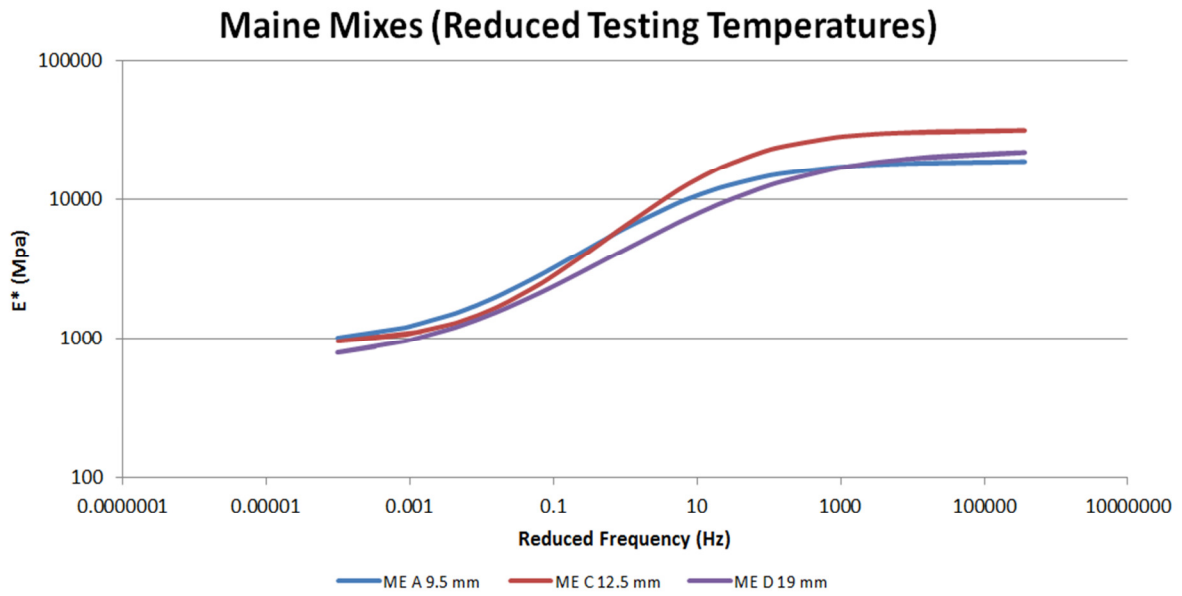
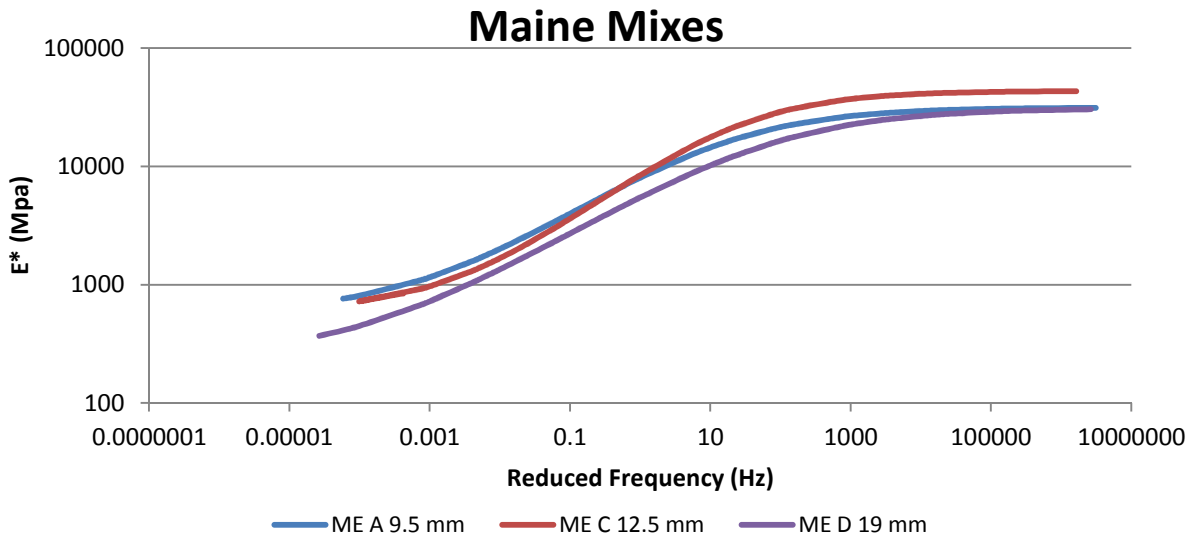
RI C M CL-1



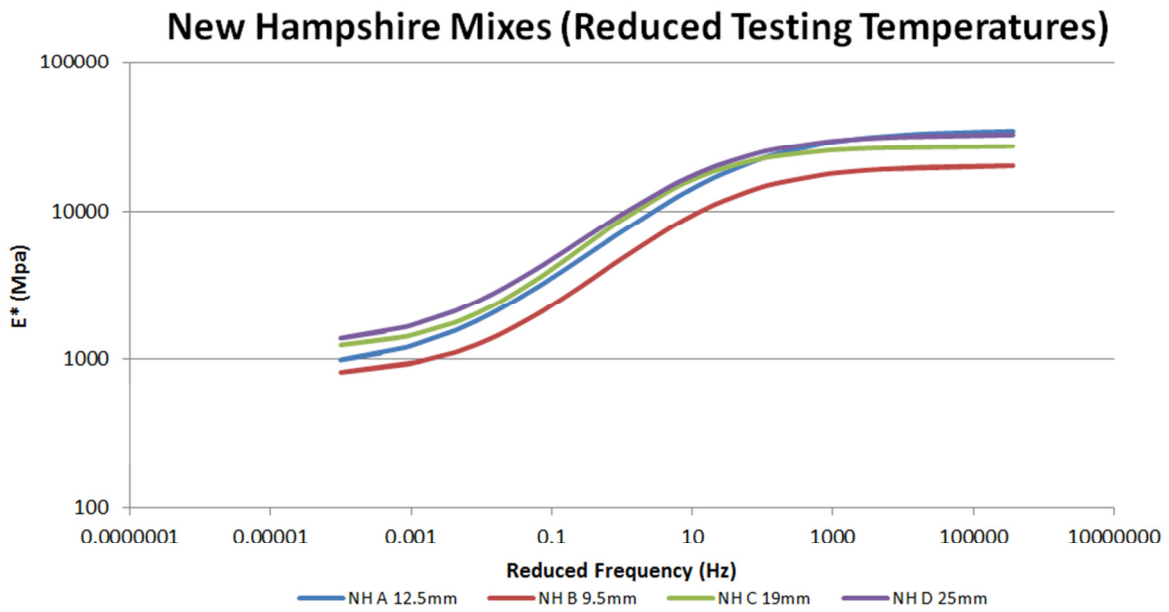
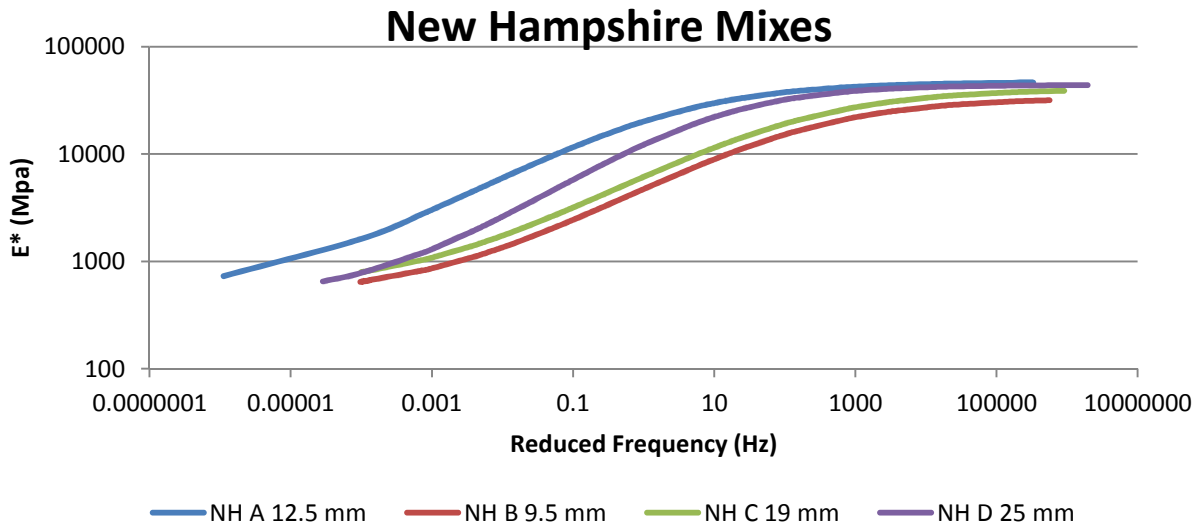
**APPENDIX B: AASHTO TP-62 MASTER CURVES VS REDUCED TESTING MASTER CURVES**



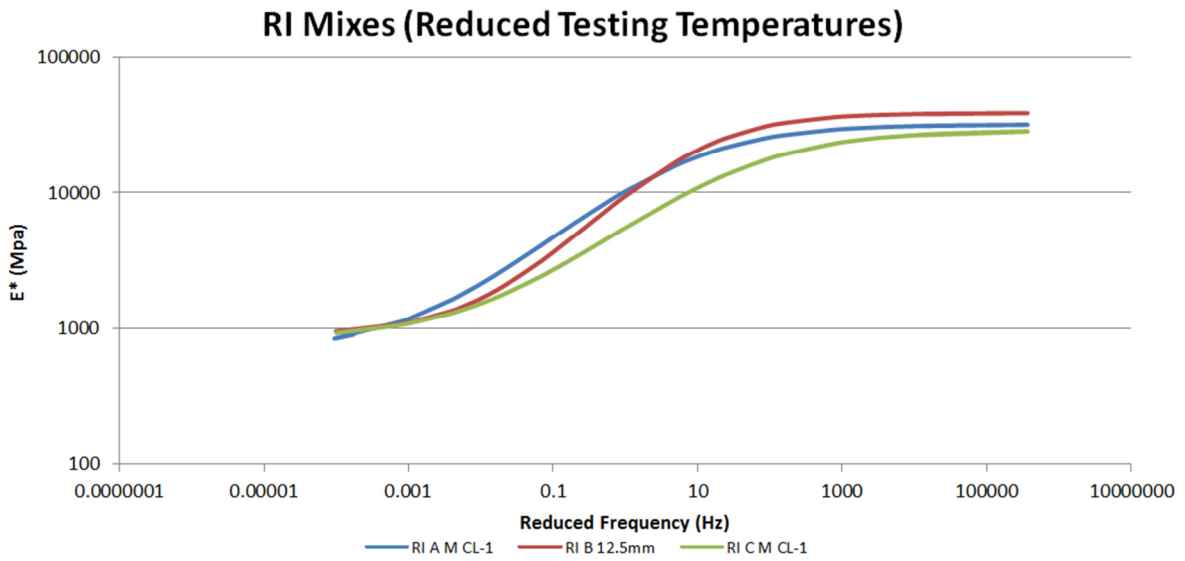
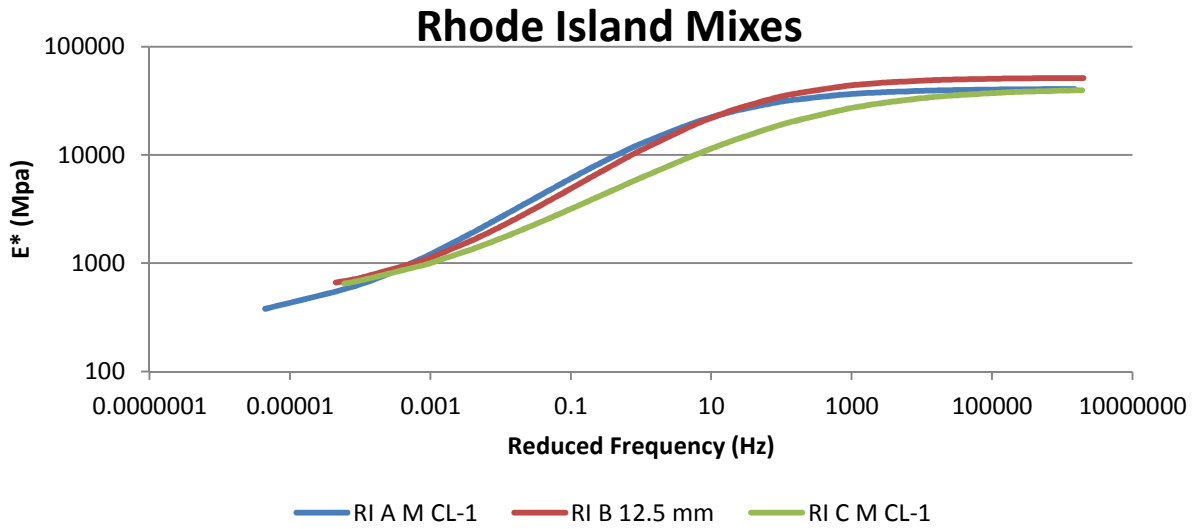
**Figure B1: Full and Reduced Testing Master Curves For Connecticut Mixes**



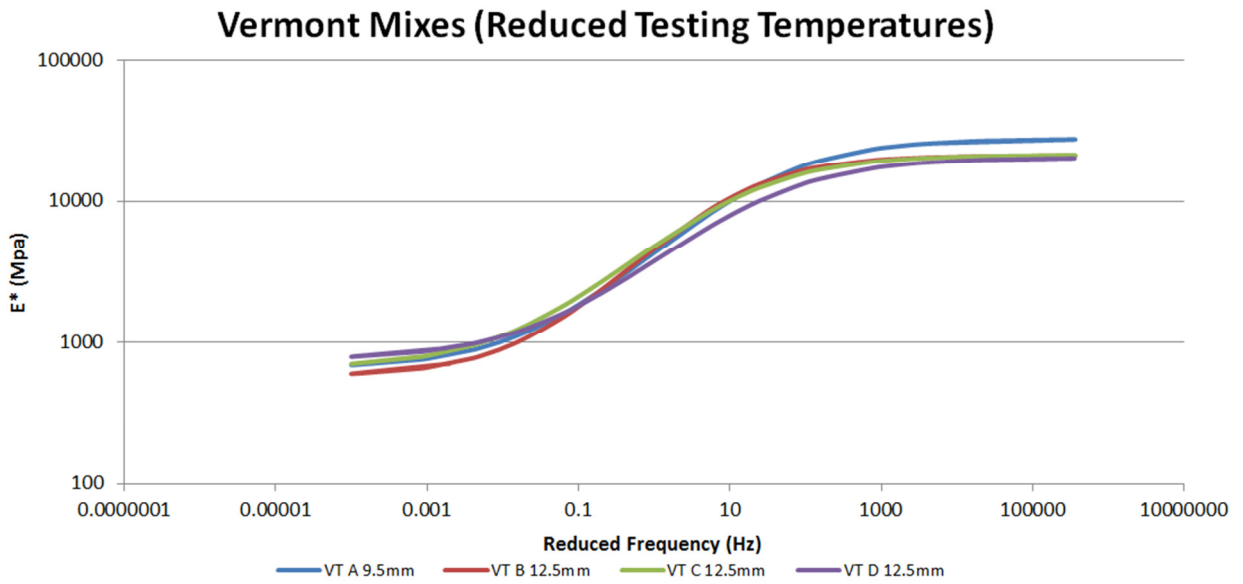
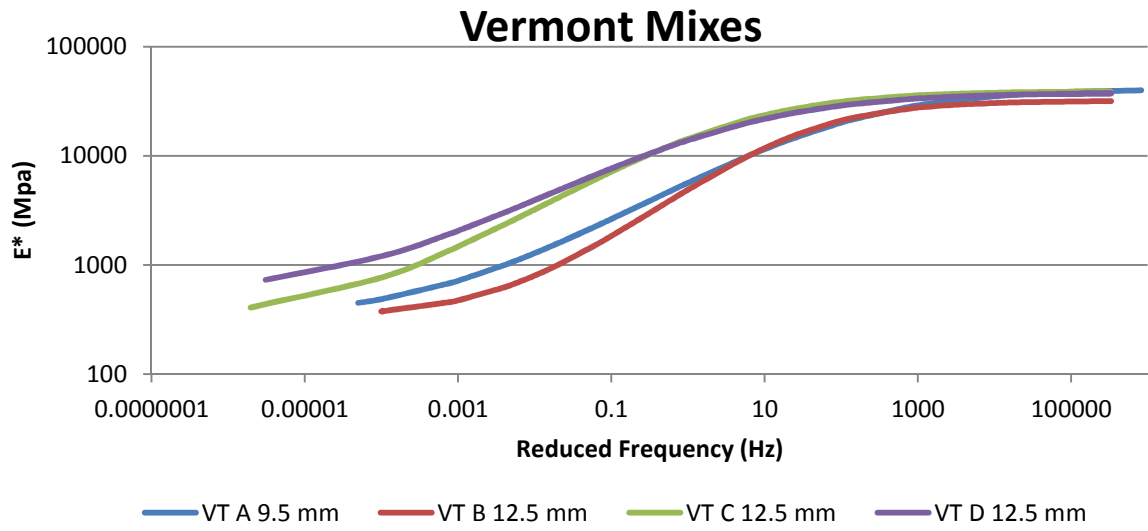
**Figure B2: Full and Reduced Testing Master Curves For Maine Mixes**



**Figure B3: Full and Reduced Testing Master Curves For New Hampshire Mixes**

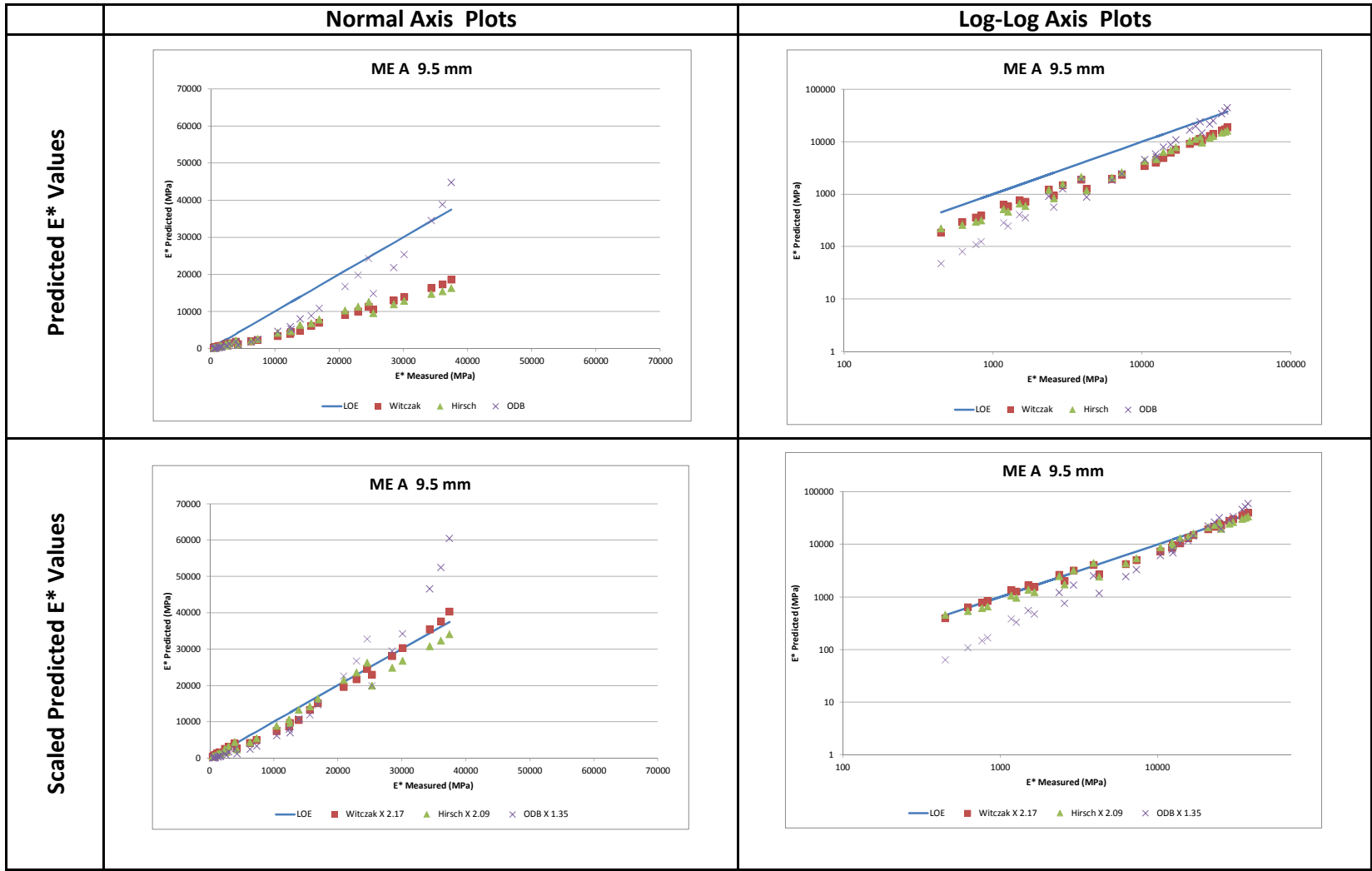


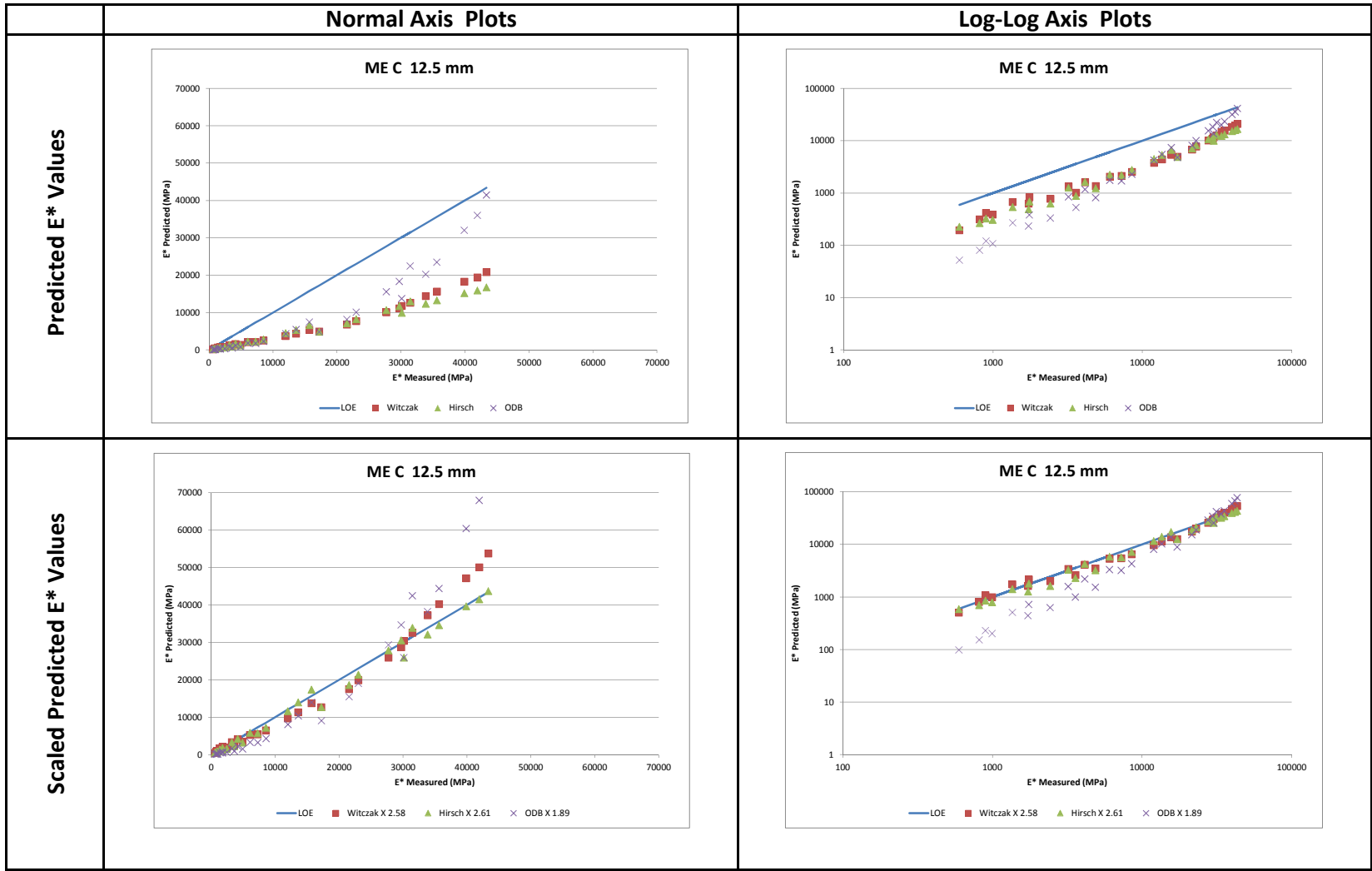
**Figure B4: Full and Reduced Testing Master Curves For Rhode Island Mixes**

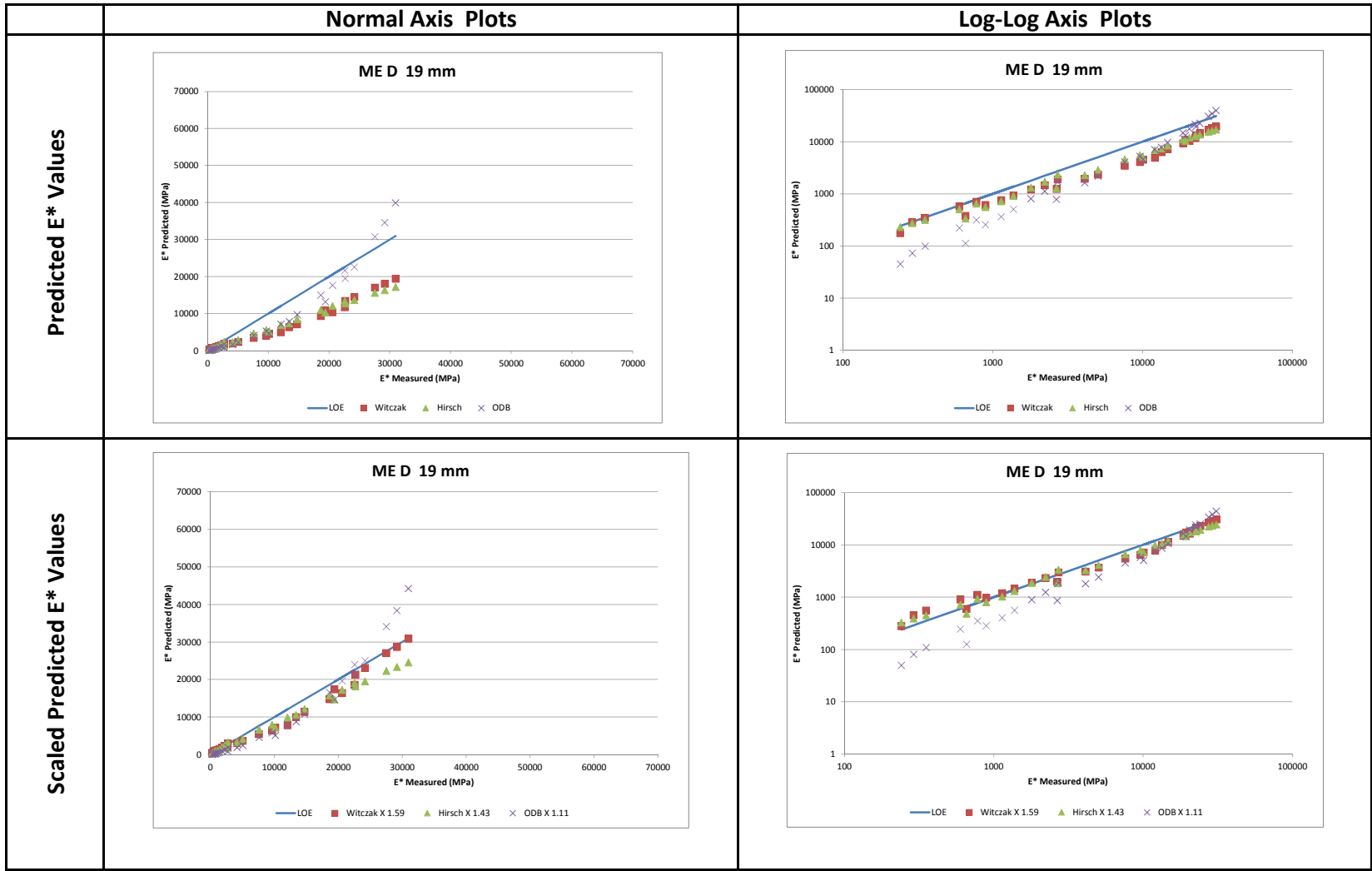


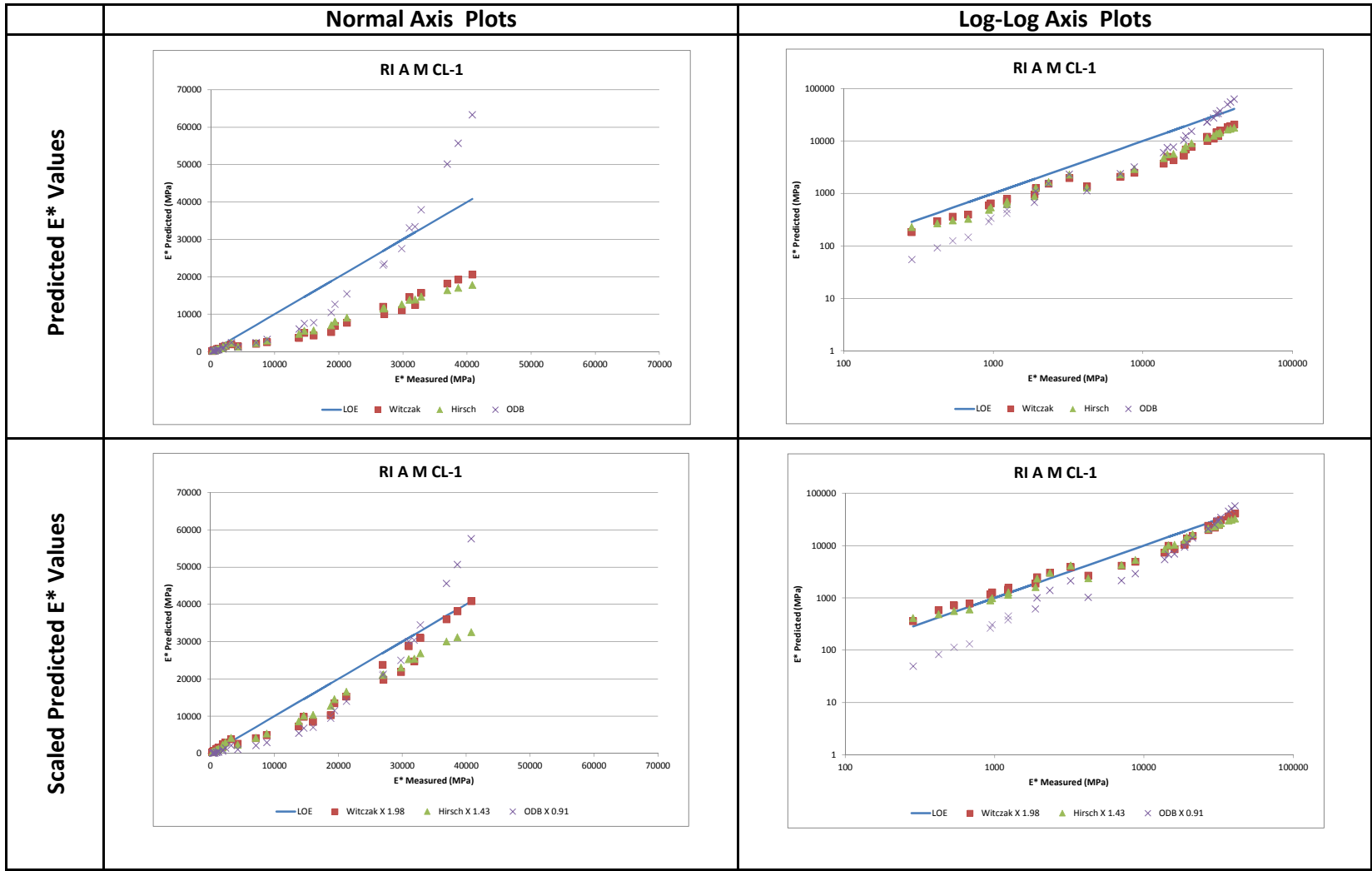
**Figure B5: Full and Reduced Testing Master Curves For Vermont Mixes**

**APPENDIX C: PREDICTED VS MEASURED |E\*|**









	Normal Axis Plots	Log-Log Axis Plots
Predicted E* Values	<p>RI B 12.5 mm</p> <p>Y-axis: E* Predicted (MPa)</p> <p>X-axis: E* Measured (MPa)</p> <p>Legend: LOE, Witczak, Hirsch, ODB</p>	<p>RI B 12.5 mm</p> <p>Y-axis: E* Predicted (MPa)</p> <p>X-axis: E* Measured (MPa)</p> <p>Legend: LOE, Witczak, Hirsch, ODB</p>
Scaled Predicted E* Values	<p>RI B 12.5 mm</p> <p>Y-axis: E* Predicted (MPa)</p> <p>X-axis: E* Measured (MPa)</p> <p>Legend: LOE, Witczak X 2.11, Hirsch X 1.95, ODB X 1.02</p>	<p>RI B 12.5 mm</p> <p>Y-axis: E* Predicted (MPa)</p> <p>X-axis: E* Measured (MPa)</p> <p>Legend: LOE, Witczak X 2.11, Hirsch X 1.95, ODB X 1.02</p>

